PEOPLE'S DEMOCRATIC REPUBLIC OF ALGERIA
MINISTRY OF HIGHER EDUCATION AND SCIENTIFIC RESEARCH
MOHAMED BOUDIAF UNIVERSITY– M'SILA

FACULTY: TECHNOLOGY
DEPARTMENT: ELECTRICAL ENGINEERING
No:

DOMAIN : SCIENCES AND TECHNOLOGY
SECTOR: RENEWABLE ENERGIES
OPTION: RENEWABLE ENERGIES IN ELECTRIAL ENGINEERING

Thesis submitted for obtaining
Academic Master's degree
By:

GHEZAL Amir

RIGUET Manal Oumaima

Entitled

Design and Optimization of a Reconfigurable Photovoltaic Generator

Defended before the jury composed of:

	University of M'Sila	Jury president
A. Benhamadouche	Univeristy of M'Sila	Supervisor
	Univeristy of M'Sila	Examiner

Academic year: 2020/2021

Abstract

In this thesis, we presented our work which is interested in the design of reconfigurable photovoltaic systems. This work allowed us to understand and overcome the different topologies that a PV generator can have. These topologies improve the behavior of a PV system in the face of the risk of malfunctions such as partial shading. The work presented is based on the dynamic optimization of the topology when the photovoltaic field is subjected to partial shading. For this, several shading scenarios are discussed and all possible reconfigurations of the photovoltaic generator are studied. An algorithm is then performed to track down and put the PV array into a configuration that reduces power loss in partially shaded conditions.

ملخص

في هذه المذكرة ، قدمنا عملنا الذي يهتم بتصميم أنظمة كهروضوئية قابلة لإعادة التشكيل. سمح لنا هذا العمل بفهم والتغلب على الهياكل المختلفة التي يمكن أن يمتلكها المولد الكهروضوئي. تعمل هذه الهياكل على تحسين سلوك النظام الكهروضوئي في مواجهة مخاطر الأعطال مثل التظليل الجزئي. يعتمد العمل المقدم على التحسين الديناميكي للطوبولوجيا عندما يتعرض المجال الكهروضوئي لتظليل جزئي. لهذا ، تمت مناقشة العديد من سيناريوهات التظليل ودراسة جميع عمليات إعادة التكوين الممكنة للمولد الكهروضوئي. ثم يتم تنفيذ خوارزمية لتعقب ووضع الصفيف الكهروضوئي في تكوين يقلل من فقد الطاقة في الظروف المظللة جزئيًا.

Résumé

Dans ce mémoire, nous avons présenté notre travail qui s'intéresse à la conception des systèmes photovoltaïques reconfigurables. Ce travail nous a permis de comprendre et de maitriser les différentes topologies que peut avoir un générateur PV. Ces topologies permettent d'améliorer le comportement s'un système PV face au risque de défaut de fonctionnement tels que l'ombrage partiel. Le travail présenté est basé sur l'optimisation dynamique de la topologie lorsque le champ photovoltaïque est soumis à un ombrage partiel. Pour cela, plusieurs scénarios d'ombrage sont discutés et toutes les reconfigurations possibles du générateur photovoltaïque sont étudiées. Un algorithme est ensuite réalisé pour traquer et mettre le GPV dans une configuration qui réduit les pertes de puissance dans des conditions partiellement ombragées.

Acknowledgement

First of all, we thank Almighty ALLAH, who has given us the courage, strength and will to carry out this modest work.

First of all, we would like to express our gratitude and recognition to Dr. A. BENHAMADOUCHE, Professor at the University of M'sila, for supervising and supporting us during the completion of this work. We also thank him for his invaluable help, the advice and the knowledge which he was able to make us benefit. It is difficult for us to express in a few words how much admiration we have for him.

Our warmest thanks to all the members of the jury, for agreeing to sit in our defense as examiners. Also, our warm thanks extend to all the engineers working at SKTM Ain El Melh for their wonderful framing and for welcoming us during professional apprenticeship.

We would like to thank our parents because this work represents a small fruit of their suffering and which without them we cannot get through these long years of study and work.

Dedications

I dedicate this modest work
to my dear parents who have supported
me throughout my life studies.
To my brother and dear sisters.
For all the family and all my friends.

Dedications

I dedicate this humble work
to my dear parents who have supported me throughout my life studies, may ALLAH preserve them.
To my dear sister and dear brothers.
To my colleague at this work.
For all the family and all my friends.
To my wonderful teacher, my loyal friend and companion, BenTaher Mounna.
To everyone who taught me even one letter.

List of tables

List of figures

Table of Contents

General introduction

Energy is an important factor for the economic growth and the development of civilization, it is the backbone of various aspects of human life. The principle current issue is how to provide continuous and constant quantity of energy through energy resources diversification. The main solution is to use renewable ressources which also aid to reduce dependency to the traditional depleted sources.

Renewable energy has become one of the most important sources of global energy outside conventional energy, as it is clean and non-polluting energy, and is characterized by automatic renewal and permanence, a large range of renewable ressources are widely exploited especialy photovoltaic energy.

The importance of photovoltaic systems lies in extending electricity to people who are in isolated areas to facilitate their lives, and to reduce fuel consumption ,also saving maintenance because once the photovoltaic panels are installed, they start their work with the highest levels of efficiency and perfection, and preserve the environment from noise pollution.

PV modules in a large array of PV generator can be connected together with different layouts, these layouts are called configurations, each configuration has its own benefits which can optimize generated power or prevent some kinds of operating fault. During normal operating mode, the performance of most PV array configurations is the same including the output power, voltage and current of the PV system. However, the PV array configuration can increase or decrease the PV output power depending on the shading pattern on the PV modules and the location of the affected PV modules. So a fully functional technology has been created for the reconfigurable PV module that was first proposed by SALAMA and ALTO in 1990 [1], which is able to dynamically change the electrical interconnection between photovoltaics as needed.

In this work, we try to design a PV system with the ability of dynamic reconfiguration. The reconfiguration of the PV array electrical connections is made with a matrix of switching circuit. The performance of the PV system is then analyzed using different configurations under different situations. In the second step of our work the optimization of the system is achieved using a specific algorithm. The configurable topologies on the photovoltaic generator is applied to increase the power production by combating shading problems,

hotspots and other problems. All topologies are applied and when a problem occurs, its structure changes dynamically to meet the requirements of the system.

This manuscript is divided in three chapter.

The first chapter present an overview of photovoltaic field, the characteristics of PV cells and their modeling is developed in order to define their operating modes. We will then study their interconnections and the security elements to be introduced when designing a PV module or field, and we will present the different categories of PV systems, we present finally usual faults and defect of a PV module.

In the second chapter, we will present the reconfigurable photovoltaic generators and their importance, and we will explain the difference between configuration and reconfiguration by presenting the characteristics and settings of each one.

In the last chapter, we will present the simulation model of the designed reconfigurable photovoltaic generator. We will create different scenarios by putting the system under different shading effects, and applying reconfiguration topologies to it. Thus, we can determine the effectiveness of the reconfiguration in improving the ability to ensure that the PV system is working at its best.

Finally, a general conclusion will be presented to summarize the main points raised in this work.

Chapter I
Photovoltaic System

I.1 Introduction

Solar energy is renewable energy produced from the sun, clean and inexhaustible; it is the most important source of energy on the planet. Direct sunlight is converted into electricity using photovoltaic (PV) converters, solar concentrating process (CSP), and many other experimental methods. Photovoltaic are widely used where electricity is generated on a large scale by solar photovoltaic arrays that produce a large amount of electricity, like the solar power generation systems are becoming more and more popular.

It is required that there be expertise, technology and competent engineers to ensure that this great energy is well used to produce electricity, within reliable and high efficiency photovoltaic systems.

In this chapter, we present generalities of photovoltaic systems, and explain how solar cell work and their properties. Also, we will present electrical and physical characteristics of PV modules, and finally then we present main faults and weaknesses of PV generators.

I.2 General information's about Photovoltaic

I.2.1 What is Photovoltaics?

Generally all photovoltaic based devices incorporate a PN junction on a semiconductor, these devices are also known as solar cells, we can briefly describe the way the solar cells work as the following, when photons (particles of light) strike some materials (semiconductors), they free electrons, which can move and create electric current, when photon pass through a solar cell, it reflect off the solar cell or be absorbed, if absorbed it can free an electron to move which creates an electric current[2].

I.2.2 PV strong and weak points

Advantages of Solar Energy:

1. Direct conversion of solar radiation into electricity
2. No mechanical moving parts, no noise, no high temperature during the conversion of energy, no pollution.
3. PV modules have a very long lifetime and a low maintenance cost.
4. The energy source, the sun, is free, ubiquitous, and inexhaustible.
5. PV is a very flexible energy source, its power ranging from microwatts to megawatts.

6. Technology in the solar power industry is constantly advancing and improvements will intensify in the future. Innovations in quantum physics and nanotechnology can potentially increase the effectiveness of solar panels and double, or even triple, the electrical input of the solar power systems.

Disadvantages of Solar Energy:

1. The initial cost of purchasing a solar system is fairly high. This includes paying for solar panels, inverter, batteries, wiring, and the installation.
2. Solar panels are dependent on sunlight to effectively gather solar energy. Therefore, a few cloudy (partial shading we will discuss about this on the next chapter), rainy days can have a noticeable effect on the energy system.
3. In off-grid situations solar energy has to be stored in large batteries. These batteries, can be charged during the day so that the energy is used at night. This is a good solution for using solar energy all day long but it is also quite expensive.
4. Uses a Lot of Space, the more electricity you want to produce, the more solar panels you will need, as you want to collect as much sunlight as possible. Solar PV panels require a lot of space and some roofs are not big enough to fit the number of solar panels that you would like to have.

I.2.3 PV Economics

The main problem and the first item on our disadvantages list is the high cost of solar cells, we can see today that the costs are actually dropping continuously and a remarkable market development has taken place. The photovoltaic world market in 2000 was 2.5 billion US dollars per year and raised until 91.3 billion dollars in 2013 as shown in Figure 1 with a 3650% growth rate in 13 years[3].

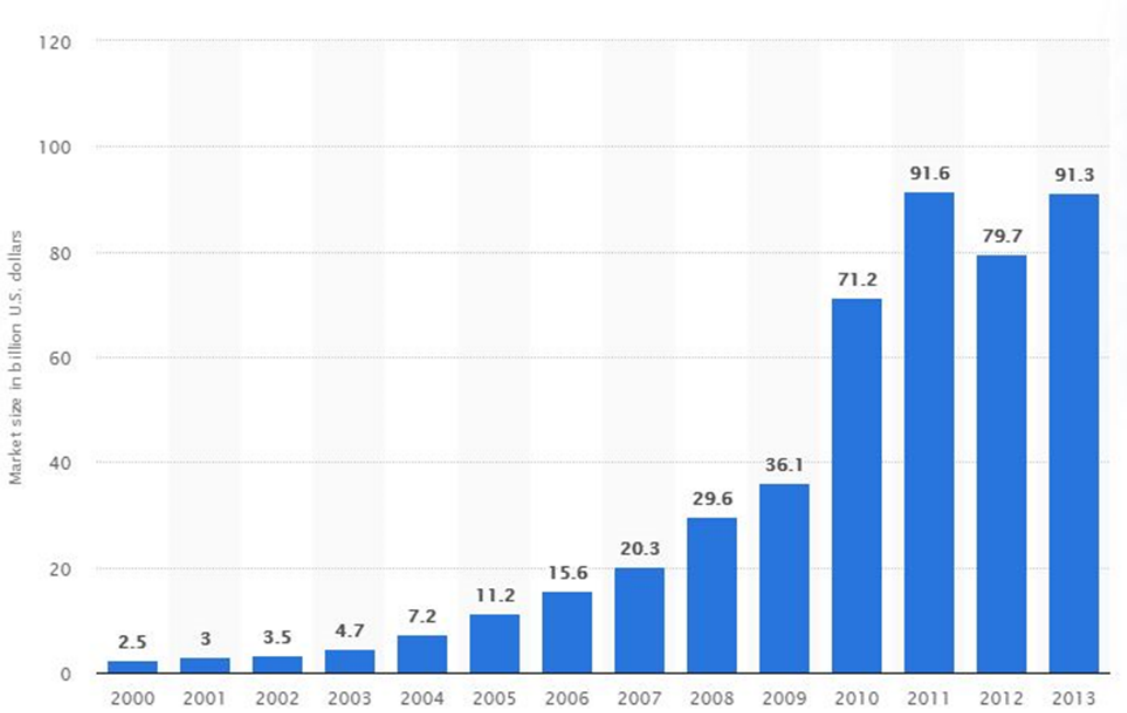

Figure 1 Solar PV market size

I.3 Solar cells

I.3.1 How solar cells work

When light occurs and absorbed by the semiconductor material, one of the properties the semiconductor must have is the ability to absorb a large part of the solar spectrum especially the visible light and this property depends on the material that the semiconductor made of.

Dependent on the absorption properties of the material, the light is absorbed in a region more or less close to the surface. When light quanta are absorbed, electron hole pairs are generated, and if their recombination is prevented, they can reach the junction where they are separated by an electric field. Even for a weakly absorbing semiconductor like silicon, most carriers are generated near the surface. This leads to the typical solar cell structure of Figure 4.

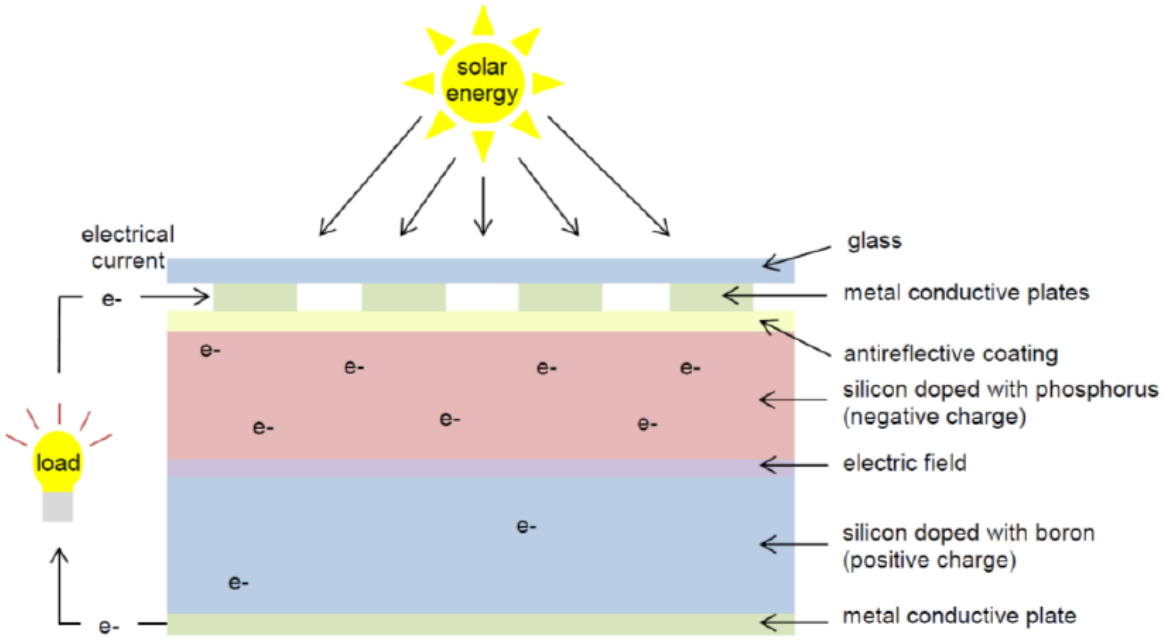

Figure 2 Typical solar cell structure

The PN junction that separates the emitter and base layer is very close to the surface in order to have a high collection probability for the photogenerated charge carriers, the thin emitter layer above the junction has a relatively high resistance which requires a well-designed contact grid[4].

I.3.2 Mechanical properties of solar cells

The dominant shape of solar cells is square-poly or mono-si, and they mostly produced in wafers, with a 155-165 mm edge (Figure 3), in the 80's solar sizes amounted to 100 mm edge length, increasing up to 125 mm around the year 2000 and to 155 mm after 2010, since then growth continued up to 155 mm.

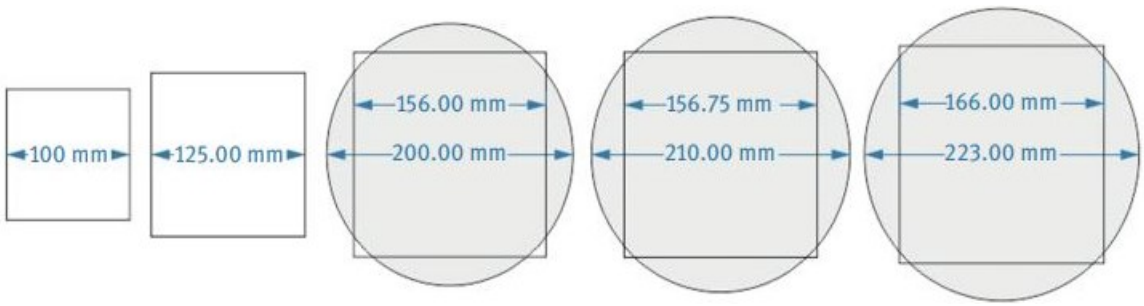

Figure 3 Solar cells size evolution

Cell thickness is expected to decrease from currently 180 μm in order to save expensive solar-grade SI material, a cell thickness of a few tens of micrometers would be enough to achieve some reasonable efficiencies[5].

I.3.3 Equivalent electric models

We can describe solar cells as an equivalent electric circuit for more profound analysis and modelling purposes, this model contains a current source and one or more diodes and resistors, which are described by circuit parameters commonly used for electronic components[6][7].

a) Single diode model

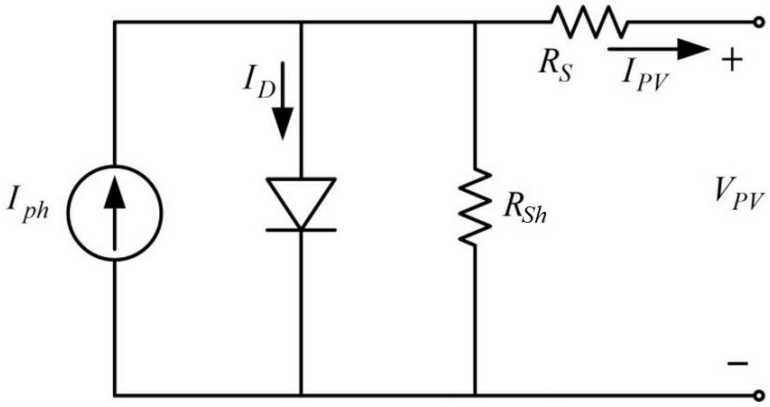

Figure 4 Single-diode model

$$I = I_0 \left[\exp\left(\frac{q(V - I \cdot R_s)}{n \cdot K_B \cdot T} \right) - 1 \right] + \frac{V - I \cdot R_s}{R_{Sh}} - I_{ph} \qquad (1)$$

Where: Iph : photocurrent,

Id : diode dark current,

Rsh, Rs : shunt and series resistances,

I0 : dark saturation current,

n : diode ideality factor,

q : elemental charge,

KB : Boltzman's constant,

T : temperature.

b) Two-diodes model

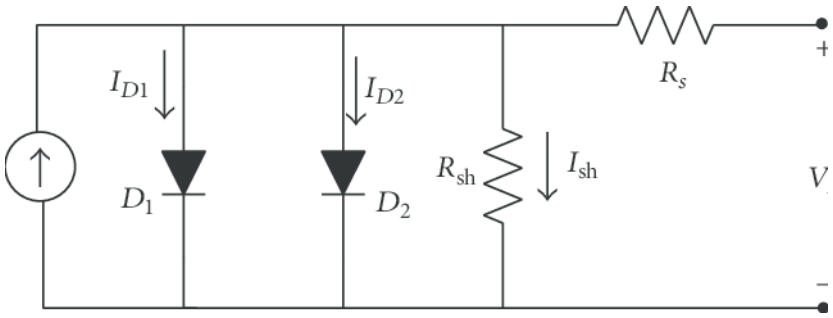

Figure 5 Two-diodes model

$$I = I_{D1}\left[exp\left(\frac{q(V - I \cdot R_s)}{n_1 \cdot K_B \cdot T}\right) - 1\right] + I_{D2}\left[exp\left(\frac{q(V - I \cdot R_s)}{n_2 \cdot K_B \cdot T}\right) - 1\right] + \frac{V - I \cdot R_s}{R_{sh}} - I_{ph} \quad (2)$$

Where: Id1 diode dark diffusion current n1=1,

Id2: diode dark recombination current n2>1.

I.3.4 Cells characteristics

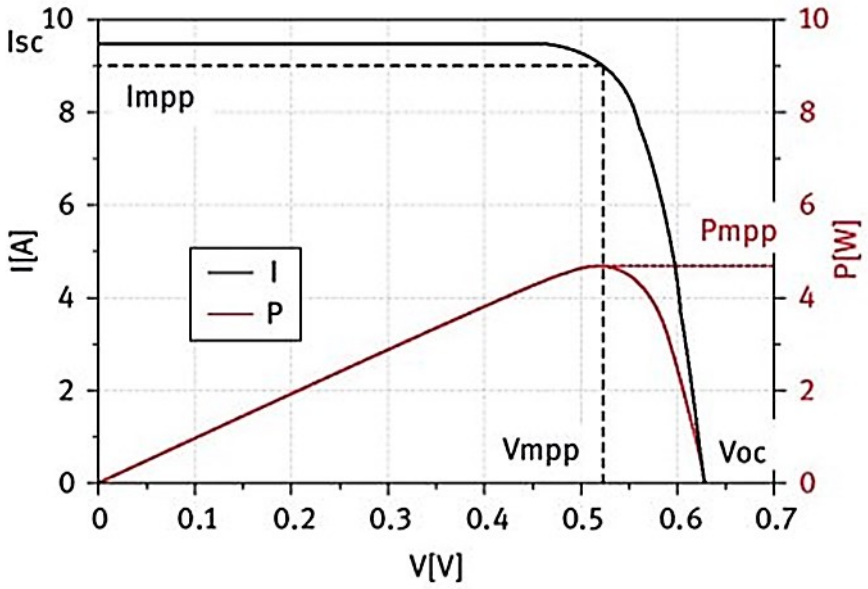

Figure 6 Current-Voltage (I-V) and Power-Voltage (P-V) curves.

The Figure 6 above describes the relation between I and V, also known as IV curve, the same figure shows a red graph also known as Power curve and it is the product of V and I,

where the peak is called maximum power point (MPP), and it indicates to Pmpp or maximum power.

Working solar cells have the parameters above and we define them as, the open-circuit voltage (Voc) and short-circuit current (Isc), Theoretically achievable Voc in modern and manufactured cells reaches 0.6-0.65 V, where laboratory cells todays can reach a maximum value of 0.75-0.8 V, The short-circuit current depends on the short-circuit current density J_{SC} and the cell area. Best laboratory J_{SC} value exceeds 40 mA/cm2.

Table 1 Calculated parameters and factors corresponding Figure 6.

I_{sc} [A]	V_{oc} [V]	I_{mpp} [A]	V_{mpp} [V]	FF	P_{mpp} [W]	η [%]
9.50	0.627	9.00	0.522	0.79	4.70	19.30%

The fill factor (FF), as defined by the equation above, is useful for the efficiency analysis of solar cells. Common industrial solar cells achieve FF values in the range of 78–80%, while high efficiency lab cells achieve 81–83%:

$$FF = \frac{V_{mpp} \cdot I_{mpp}}{V_{oc} \cdot I_{sc}} = \frac{P_{mpp}}{V_{oc} \cdot I_{sc}} \qquad (3)$$

Where: FF fill factor,

V_{mpp} maximum power point voltage (V),

I_{mpp} maximum power point current (A),

V_{OC} open-circuit voltage (V),

I_{SC} short-circuit current (A),

P_{mpp} maximum power (Watts).

The efficiency η of a solar cell is defined as the ratio of the delivered electric power (W) at the MPP to the radiant flux on the full cell area under a defined irradiance as described in the next equation:

$$\eta = \frac{P_{mpp}}{\Phi_e} = \frac{P_{mpp}}{E \cdot A_{cell}} \qquad (4)$$

Where: Φe radiant flux (Watts),

P_{mpp} maximum power (Watts),

A_{cell} cell area (m^2),

E irradiance (W/m^2).

The conversion efficiencies η of today's production cells are in the range of 13% to 16%, but module efficiencies are somewhat lower. The best laboratory efficiency of crystalline silicon achieved so far is 24.7%, which approaches the theoretical limit of this type of solar cell[8].

I.4 PV systems

I.4.1 PV systems components

a. Mounting structure it could be mobile or fixed with an angle, this structure directs the solar panels toward the sun

b. Energy storage, usually batteries, it is a vital part of off-grid systems, because it assures that the system can deliver electricity during night or bad weather

c. DC/DC converters, buck or boost converters helps to control the module output, which will have a variable voltage depending on the time of the day and weather conditions, to a compatible output voltage that can be used as input for an inverter in a grid connected system

d. Inverters that are used in grid-connected systems to convert the DC electricity originating from the PV modules into AC electricity that can be fed into other devices or transformers

e. Charge controllers that are used in stand-alone systems to control charging and often also discharging of the battery

f. Electric load or transformers, both of them are not really a part of the PV systems itself, transformers help to boost the voltage output from inverters to be easily transported with smallest losses.

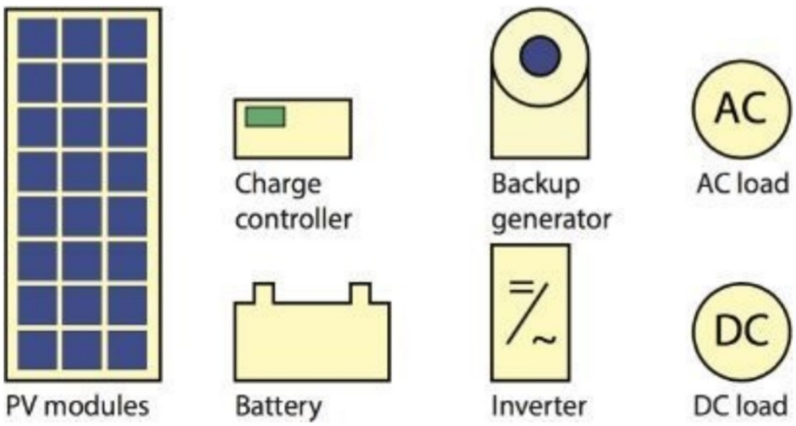

Figure 7. Different components of a PV system.

I.4.2 Stand-Alone PV Systems

Stand-Alone, off-grid or grid-independent systems, rely on solar power only, theses systems can consist of the PV modules and a load only (simple off-grid system), or in most cases they include batteries for energy storage (complex off-grid system).

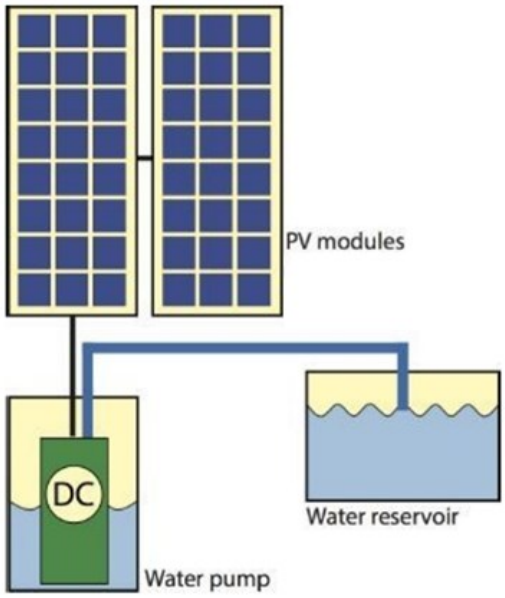

Figure 8 Simple off-grid system without energy storage.

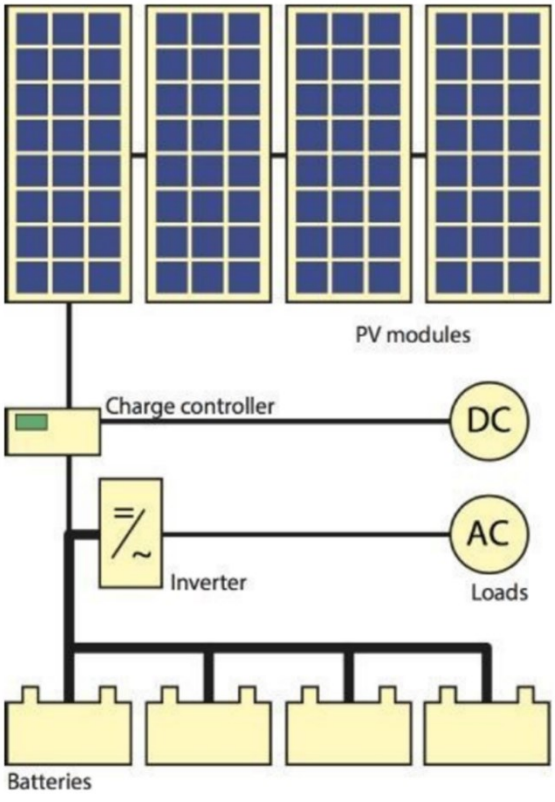

Figure 9 Complex off-grid system including energy storage.

I.4.3 Grid-Connected PV Systems

Grid-connected PV systems they are connected to the grid via inverters and transformers, in small systems such as those installed in residential homes, the inverter is connected to the distribution board, these systems do not require energy storage components since they are connected to the grid.

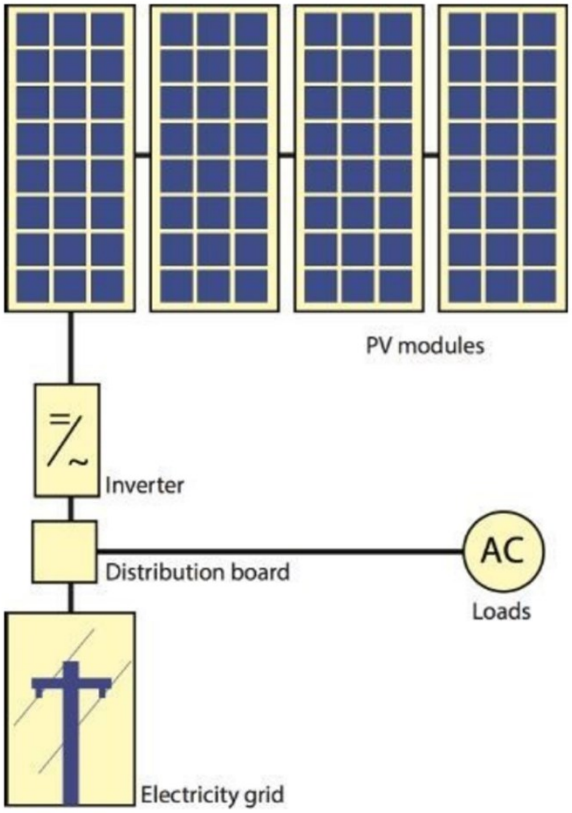

Figure 10 Grid-Connected PV System schematic.

I.4.4 Hybrid Systems

Hybrid systems combine PV modules with a complementary method of electricity generation such as a diesel or gas as an alternative electricity source (often called backup generators), these systems are rarely used due to its high cost.

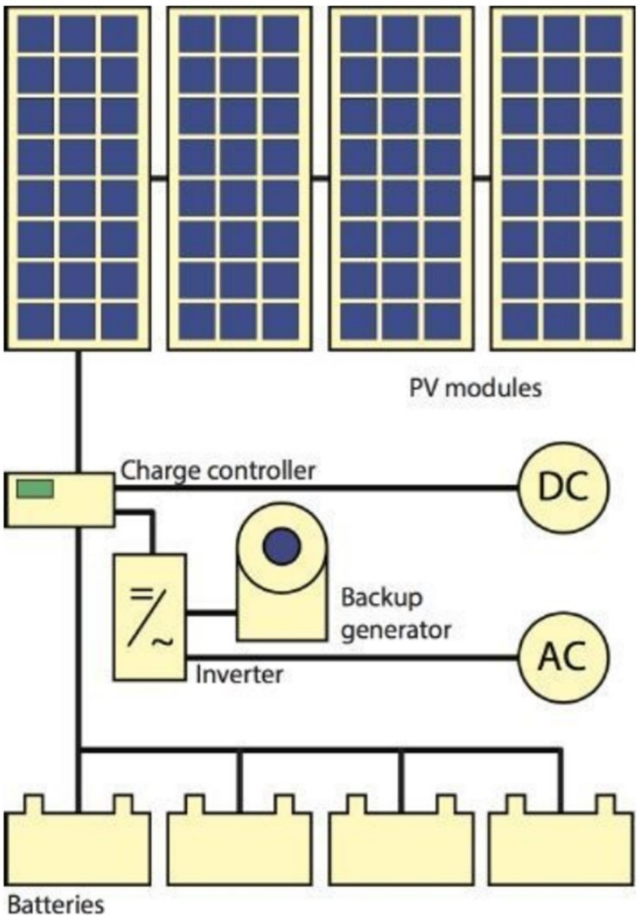

Figure 11 Hybrid PV system with a backup generator schematic.

I.5 PV Modules

I.5.1 Definition

The maximum voltage the silicon solar cells can generate is up to 0.5 volt due to today's technological limits, and making a cell larger does not increase its voltage and, although a cloud passing overhead doesn't significantly reduce the output voltage of a solar cell, the current produced is strongly affected by the level of light hitting the cell (partial shading for example and we will discuss this situation in the next chapter), also a voltage of 0.5 is too low to be useful, so a number of solar cells are commonly wired together, connecting them in Series or Parallels to produce a PV module[9].

For practical applications, a large number of solar cells are interconnected and encapsulated into units called PV modules, which is the product usually sold to the customer.

I.5.2 Modules configurations

As described in previous section we defined PV modules as the ensemble of solar cells wired together in various configurations series or parallels or both mixed, we can connect the solar cells in different ways.

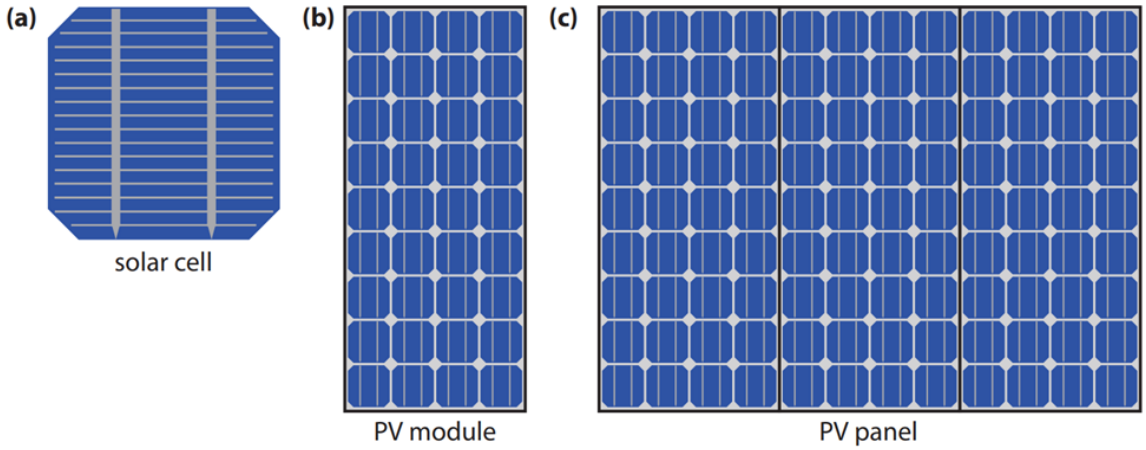

Figure 12 Solar cell, PV module and PV Panel

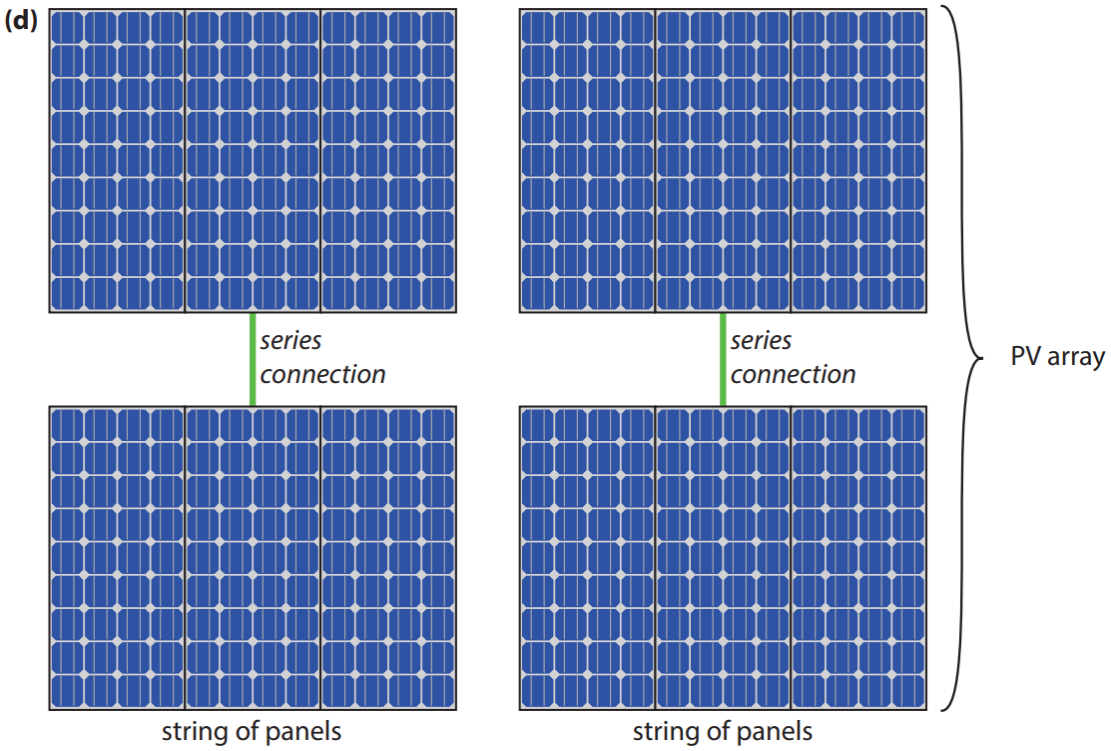

Figure 13 PV array contains 2 strings, each string have 2 panels connected in series

In series connection as shown in Figure 14 (a), the voltages added up, for example, if the open circuit voltage of one cell is equal to 0.6 V, a string of three cells will produce an open circuit voltage of 1.8 V (0.6+0.6+0.6 = 1.8 volts).

In Figure 14 (b) series connected cells, the current do not add up but the current of the whole string is determined by a one cell, that cell produces the smallest current, in general we can conclude that the total current in a string of solar cells is equal to the smallest current generated by one single solar cell.

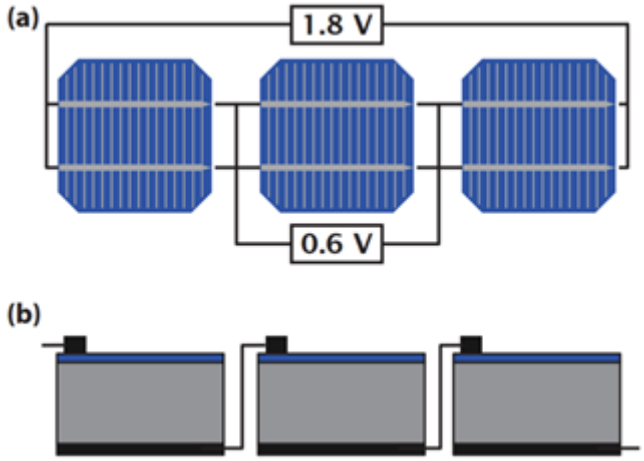

Figure 14 (a) the output of 3 and 1 cells connected in series (b) 3 cells in series.

We can connect solar cells in parallels as shown in Figure 15, the opposite of series connection is the parallel connection, in this type of connection the voltage is the same across all solar cells, while the current add up, For example, three cells connected in parallel the current becomes three times larger ($I1 = 1, I2 = 1, I3 = 1, I = I1 + I2 + I3 = 3\ Amps$).

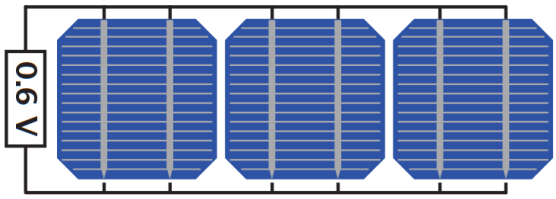

Figure 15 Three solar cells connected in parallel.

I.5.3 Modules characteristics

Like solar cells, PV modules are often characterized by short circuit and maximum power point currents, Figure 17 (a) shows a PV module contains 40 solar cells connected in series, if one cell has a short-circuit current of 2 A, and an open-circuit voltage or 0.6 V, the module would produce an output of $Voc = 40 \times 0.6 = 24\ V$ and $Isc = 2\ A$

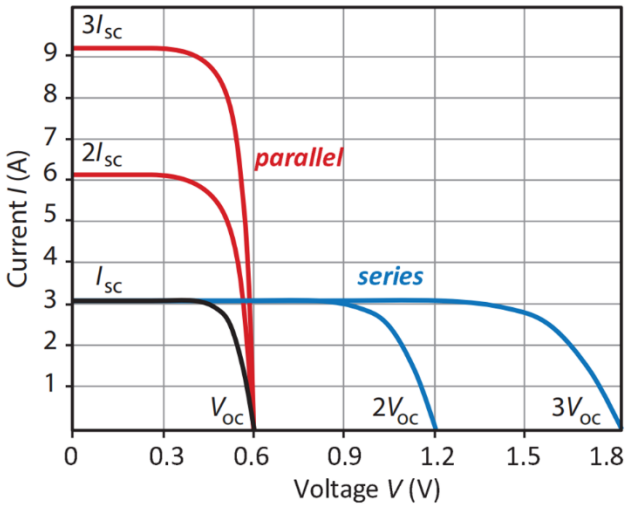

Figure 16 IV curves of solar cells connected in series and parallels

If two strings of 20 series connected cells are connected in parallel as shown in Figure 17 (b), the output of the module will be $Voc = 20 * 0.6 = 12\ V$ and $Isc = 2.5 = 10\ A$.

By those calculations we can prove that IV characteristics of a module consisting of *m* identical cells in series and *n* identical strings in parallel, the voltage multiplies by a factor *m* while the current multiplies by a factor *n*.

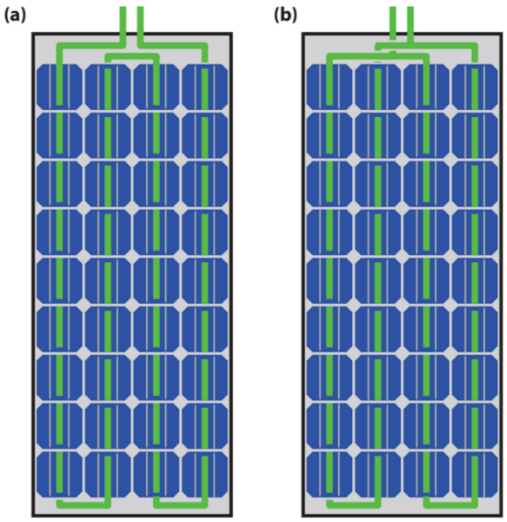

Figure 17 PV module contains (a) a string of 36 cells connected in series (b) two strings each of 18 cells connected in parallel

I.5.4 PV Modules basic protection with diodes

We can define diodes as a complicated semiconductor devices or components that allows the current to flow in a single direction, in Figure 18 we distinguish 6 diodes installed in 2 different ways, the 3 green diodes installed in parallel is a Bypass diode, the other 2 red diodes are Blocking diodes[10].

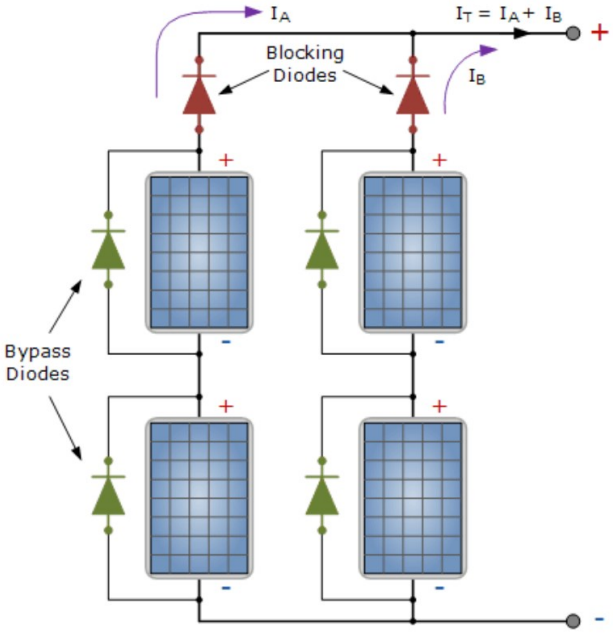

Figure 18 PV array contains 4 modules each with a 1 bypass diode

Bypass diodes installed in parallel with the module or in some group of cells those diodes perform the function of providing a bypass path for the current to flow around the bad, overheated, shaded cell or module.

Blocking diodes also called a series diode or isolation diode, ensure that the electrical current only flows in one direction of the series array to the external load, controller or batteries, the reason for this is to prevent the current generated by the other parallel connected PV panels in the same array flowing back through a weaker (shaded) network and also to prevent the fully charged batteries from discharging or draining back through the array at night. So, when multiple solar panels are connected in parallel, blocking diodes should be used in each parallel connected branch[11].

I.5.5 PV Modules faults and defections

In the table below, we present a review on the most important and common defect observed in the photovoltaic modules, these defects are originating from modules functioning and from its own mechanical structure[12][13].

Table 2 PV Modules faults and defections

Defect	Possible reason	Effect on PV module
Faults found in all PV modules		
Delamination	Problem of adhesion between the glass, encapsulant, active layers, and back layers, caused by contamination or environmental factors	Humidity ingress, corrosion, reduced module performance, isolation fault
Back sheet adhesion loss	Mechanical stress, UV radiation, heat, humidity	Corrosion, mechanical stress, risk of electric arcs
Junction box failure	Poor fixing, poor manufacturing, bad wiring	Higher resistance, risk of thermal damage
Frame breakage	Snow loads or other mechanical loads and extreme weather conditions	Humidity ingress, reduced module performance, isolation faults
Cell cracks	Mechanical stress induced by mechanical or thermal loads	Insulated cell areas, reduced module performance
Broken interconnection	Mechanical stress induced by mechanical or thermal loads	Higher resistance, insulated cells, and strings, risks of hot

		spots
Light-induced power degradation (LID)	Light exposure	Reduced module performance
Faults found in thin-film PV modules		
Micro arcs at glued connectors	Problems in the manufacturing process (lack of pressure on the connection area in the conductive gluing)	Reduced module performance (affects mainly the FF of the I-V curve)
Shunt hot spots	Problems in the manufacturing process, reverse bias operating of cells (caused by shading or soiling)	Hot spots, reduced module performance, glass breakage, loss of mechanical stability
Back contact degradation	Poor manufacturing, high temperatures, prolonged open-circuit conditions	Reduced module performance

I.6 Conclusion

In this chapter, we presented generalities about photovoltaic energy, its origins and economic study, then we explained the principle of operation of the solar cell and its characteristics. We showed that the PV cell has a non-linear I(V) characteristic and that it can be modeled by a simple electrical circuit.

Then we presented photovoltaic systems with an explanation of their types and individual characteristics. Also, we have defined photovoltaic units and their methods of connection either in series or on the branch, then we presented the characteristics of each arrangement. Finally, we finalized this chapter by talking about the defects that occur in the photovoltaic module during their life cycle operation.

Chapter II
Reconfigurable Photovoltaic Generators

II.1 Introduction

The traditional interconnection of PV cells inevitably involves losses related at least to dispersions, however small, of the electrical characteristics. Within a module, these phenomena are known in the literature as "mismatch". On the other hand, in the event of shading, this type of connection has weaknesses that are partially offset by the presence of bypass diodes[14].

In order to generally avoid this type of power loss in a module or a photovoltaic field, it is necessary to treat this arrangement actively, opening up more solutions to the power produced to be extracted. Thus, when it is subjected to partial shading or a failure of a cell, a more complex connection system inserted in the PV module can solve both the losses of producible, avoid local heating which in the long run can reduce lifespan, make the insertion of a PV module easier, especially in urban areas that were previously difficult to explore due to relatively poor quality of sunlight. Thus, the new distributed production PV module will notably have to produce more power than a conventional PV module while offering very high reliability guarantees. Pushing to the extreme, the use of reconfigurable architectures makes it possible to rearrange the position of the modules at will, going so far as to disconnect from the producible one or more groups with too low power when shading occurs.

II.2 Presentation of reconfigurable generators

The photovoltaic array reconfiguration is one of the solutions for electrical mismatch losses in PV systems, such that reconfigurable systems change the inter-connections between the solar modules in a solar PV array.

The reconfigurable PV array was first proposed by Salameh et alto start [1] and operate permanent magnet DC motor coupled to volumetric water pump. Then it was proposed to start and accelerate electric cars using a number of PV modules [1]. Sherif and Boutros [1]proposed a reconfiguration scheme for PV modules using transistors as switches between cells. Nguyen and Lehman [1]used reconfiguration inside PV arrays and proposed two reconfiguration algorithms. However, they did not propose any mathematical formulation for the optimal reconfiguration. They also proposed dividing the PV array into fixed and adaptive parts with a switching matrix between them. They used one column only as an adaptive part in order to reduce the number of sensors and switches which can make the scheme ineffective if the shaded area is large.

Also, Velasco et al. [1]used reconfiguration for grid connected PV arrays and proposed a mathematical formulation for it. Moreover, they proposed the irradiance equalization index as the difference between the maximum and the minimum average row irradiance levels in the array.

II.2.1 Reconfigurable modules

As we know, it is difficult to place integrated PV modules in ideal conditions. Therefore, imperfect orientation and inhomogeneous radiation from shading from obstructions often create non-uniform illumination which creates a current mismatch between the different PV modules as well as between the different cells that make up each PV module, which in turn leads to a decrease in the total capacity of the PV module. So, a new fully functional technology has been created for the reconfigurable smart PV module, which is able to dynamically change the electrical interconnection between photovoltaics. [15]

II.2.2 Reconfigurable panels

The connections between groups of cells (cell-strings) can be rearranged in order to increase the overall power output. In a traditional PV panel, current mismatch between the series-connected cells limits the generated power output by either reducing the overall current or by bypassing the substring containing the limiting cells. A reconfigurable panel respond to such a situation by changing the connections to a more favorable configuration, allowing the majority of the cells to operate.

II.2.3 Interests

Reconfigurable systems have the ability to change their configurations depending on the operational conditions. This concept is beneficial for the systems in which the configurations are easily convertible. The introduction of reconfigurability enhances system reliability, capacity together with further system developments.

Reconfigurability can be introduced to a power system at the hardware level as well as in the control level to adapt to the on-demand functional requirements through changing its hardware topology or control methodology. The reconfiguration method in monitoring systems allows for predicting the most suitable configuration for a specified period and for smart management of the PV network. Different reconfigurable solutions are available for different sections of standalone solar PV systems such as PV array, power conversion unit and PV connected microgrids, Features of solar PV microgrid over a solar home system.

Series and parallel connections are the basic configurations used to provide the required power output. The other configurations are modified versions of the base configurations designed to reduce the effect of partial shading while providing the same power output as the base configurations.

Reconfigurable PV system a new concept for a single-phase which is equipped with a quasi-source inverter is proposed to maintain an un-interrupted power supply to the loads in a case of grid failure.

II.3 Configuration and reconfiguration

II.3.1 Configuration

PV modules can be connected in different PV array configuration. During normal operation mode, the performance for most PV array configurations are the same including the output power, voltage and current of the PV system. However, the PV array configuration could increase or decrease the PV output power depending on the shading pattern on the PV modules and the location of the affected PV modules

II.3.1.1 Serial Connection

All PV modules are connected in series as shown in the figure1, although a series configuration may increase the output voltage, if the modules experience partial shading or malfunction, the overall voltage output drops substantially[16] [15].

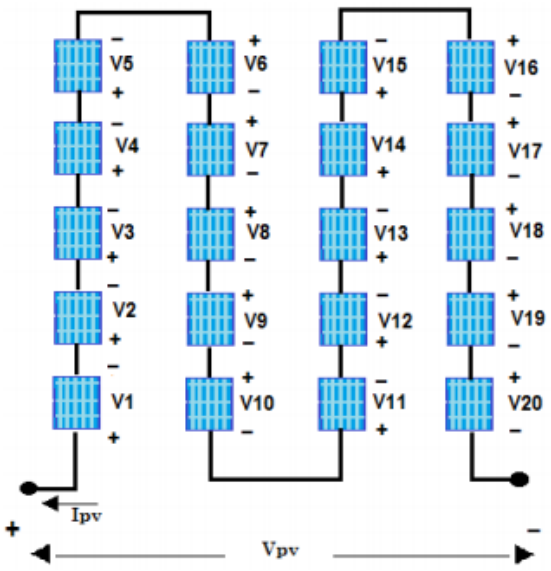

Figure 19 Serial Connection

II.3.1.2 Parallel Connection:

All PV modules are connected in parallel as shown in Figure 20, although a parallel configuration may increase the output current of the module, if any modules experience partial shading or malfunction, the overall current output decreases[16][15].

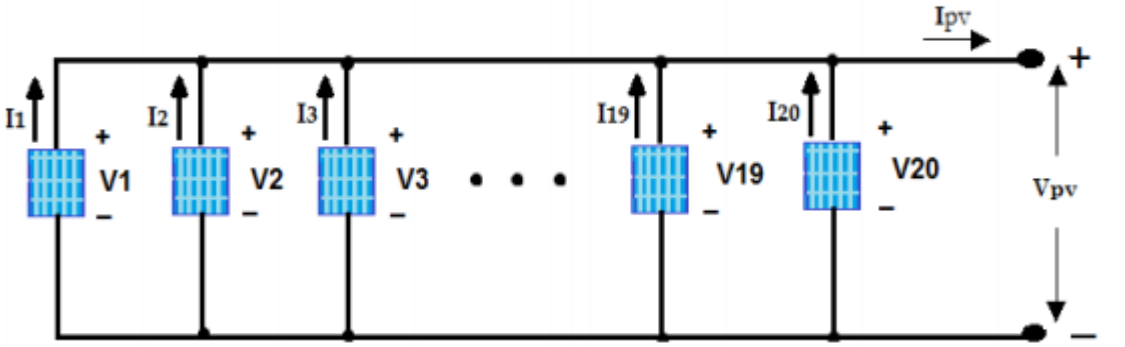

Figure 20 Parallel Connection

II.3.1.3 Parallel Serial Configuration (SP)

The circuit of the SP configuration is shown in Figure 21. The field has four strings (branches) in parallel, each contains six modules connected in series[16][15].

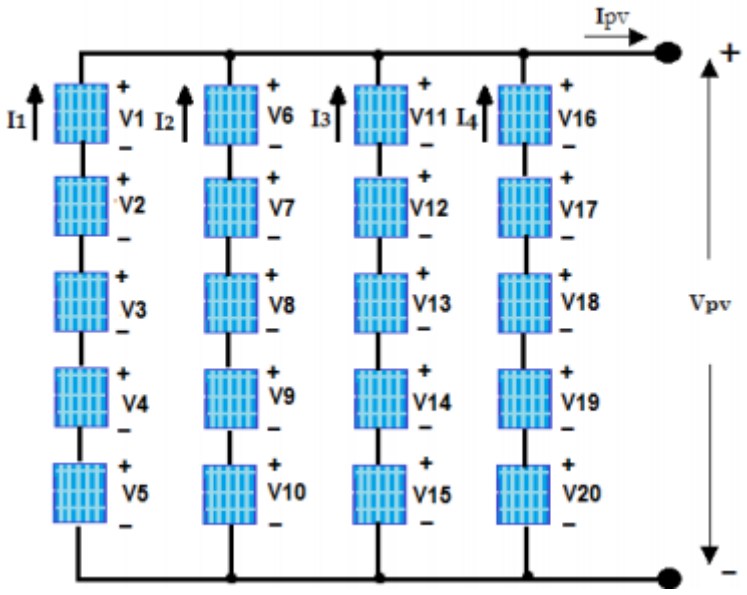

Figure 21 Configuration SP

II.3.1.4 Totally Cross-Tied Connection (TCT)

All PV modules are connected in series then crossed in parallel as shown in Figure 4, this configuration involves a scheme in which the modules are connected in parallel and then in series. Several PV modules are first connected in parallel, then its parallel modules are then

connected in series, this connection diagram can solve the drawbacks of serial and parallel arrangement[16][15].

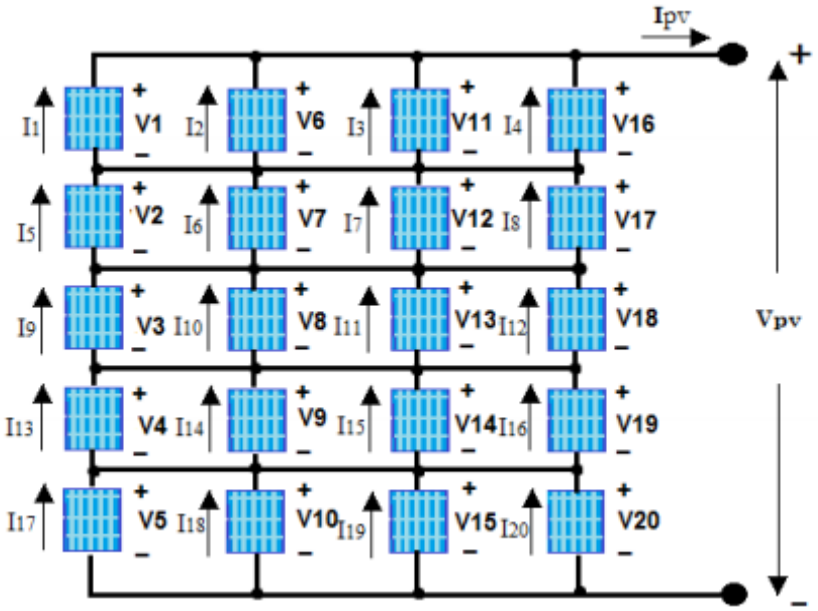

Figure 22 Totally Cross-Tied Connection (TCT)

II.3.1.5 Bridge Linked configuration (BL)

The configuration (BL) is shown in the figure below composed of several repetitive stitches. Each stitch is made up of four modules of two adjacent strings, linked together by connections[16][15].

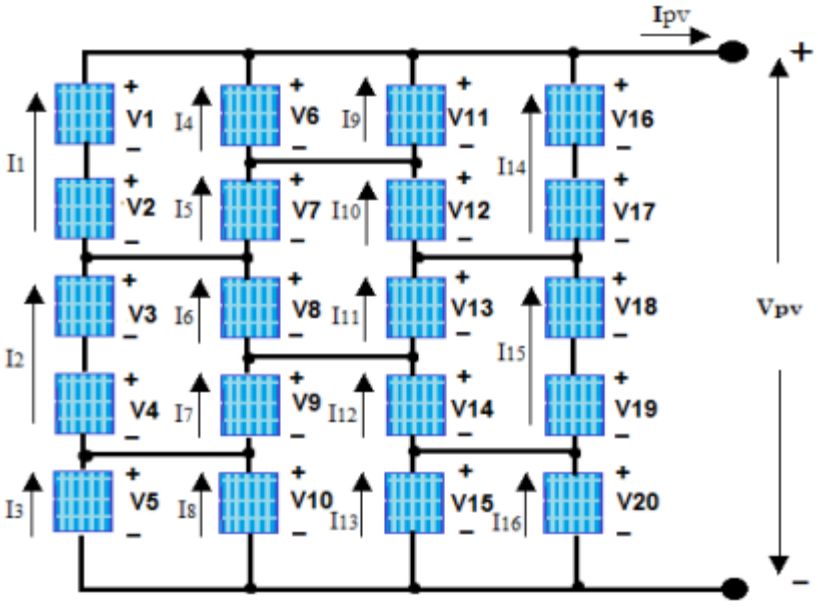

Figure 23 Configuration BL

II.3.1.6 Honey Comb configuration (HC)

The Honey Comb (HC) system circuit is inspired by the shape hexagonal of the honeycomb as shown in Figure 24[16][15].

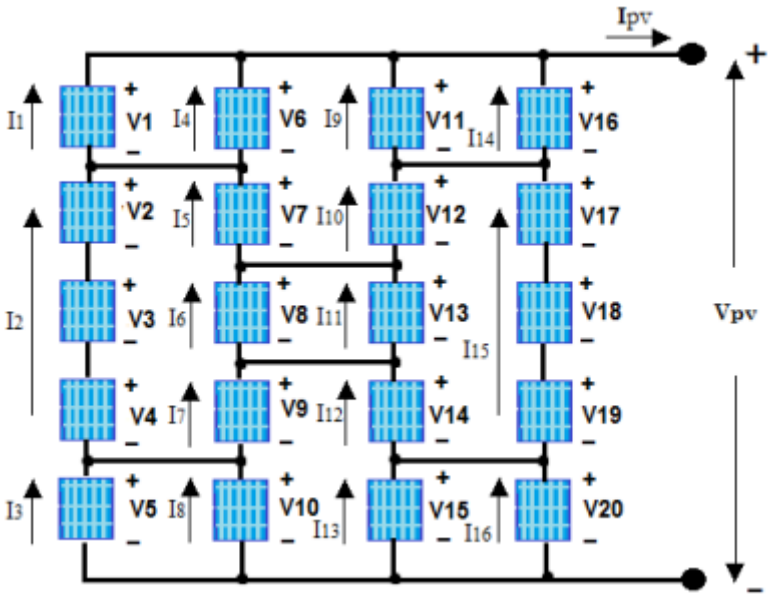

Figure 24 Configuration HC

II.3.2 Reconfiguration

Reconfigurable systems have the ability to change their configurations depending on the operational conditions[17]. This concept is beneficial for the systems in which the configurations are easily convertible

Today, most of the power system components do not solely come up with hardware such that these components are interconnected with different controlling and monitoring systems. Existing traditional approaches are no longer sufficient to meet the evolving controlling and monitoring requirements of the modern systems. A modern power system requires a dynamic wide-area view, fast and predictive analytics and system wide coordination. Therefore, moving towards reconfigurable power system components is the solution to fulfil future requirements[18]. Reconfigurability can be introduced to a power system at the hardware level as well as in the control level to adapt to the on-demand functional requirements through changing its hardware topology or control methodology.

Different reconfigurable solutions are available for different sections of PV systems such as PV array, power conversion unit and PV connected microgrids, and the synthesis of those configuration schemes are presented in Figure 25.

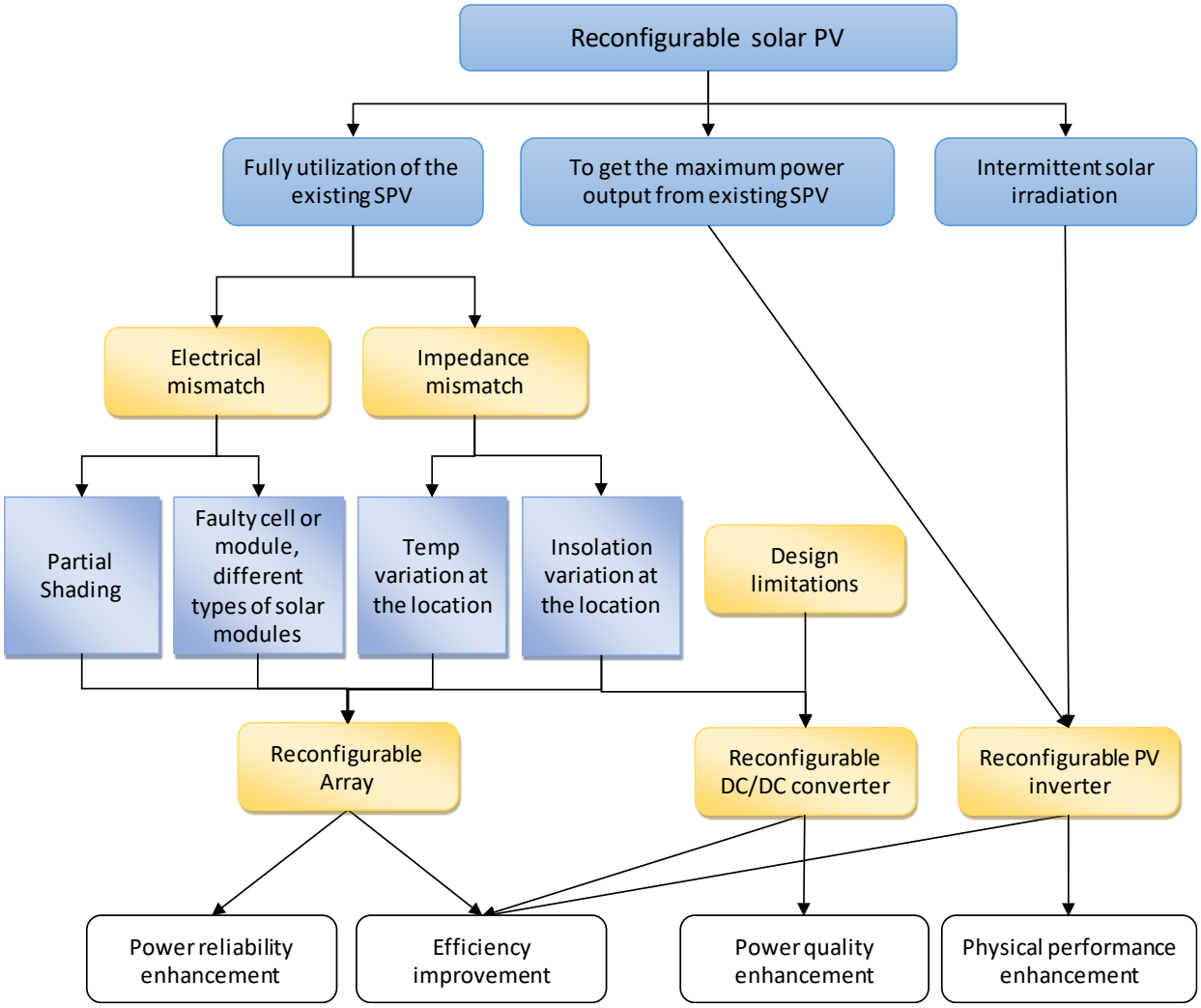

Figure 25 Summary of the application of reconfigurable solar PV systems

1. **The reconfigurable operation for solar PV array**
2. **The reconfigurable operation for solar PV array**
3. **Reconfigurable microgrids**

II.3.2.1 Reconfigurable solar converter

A new concept called Reconfigurable Solar Converter (RSC) is under development [19].It is a conventional 3-ph SPV converter, with a minimum modification to the utility-scale. Its system configuration is an SPV plant type with a battery backup. This system consists of an SPV array, a battery backup, a conventional 3-ph inverter, a harmonic filter, a transformer and additional switches.

Here, the reconfigurable unit is a single-stage power conversion unit and its controllability has been improved to change its configurations according to the requirements of the grid and the battery, and the availability of SPV generation. The proposed power conversion unit has the ability to operate in five major modes of operations through additional switching. These modes are:

- PV to the grid - SPV provides power supply to the grid.
- PV to the battery - SPV provides power supply for the charging of the battery.
- PV-Battery to the grid - Both SPV and battery supply power to the grid.
- Battery to the grid - Battery is sending power to the grid.
- Grid to the battery - Battery is charging from the grid supply.

Here, reconfiguration is proposed to improve the power conversion efficiency compared to the dual-stage power converter and to maximize the utilization, whenever the peak shifting is required.

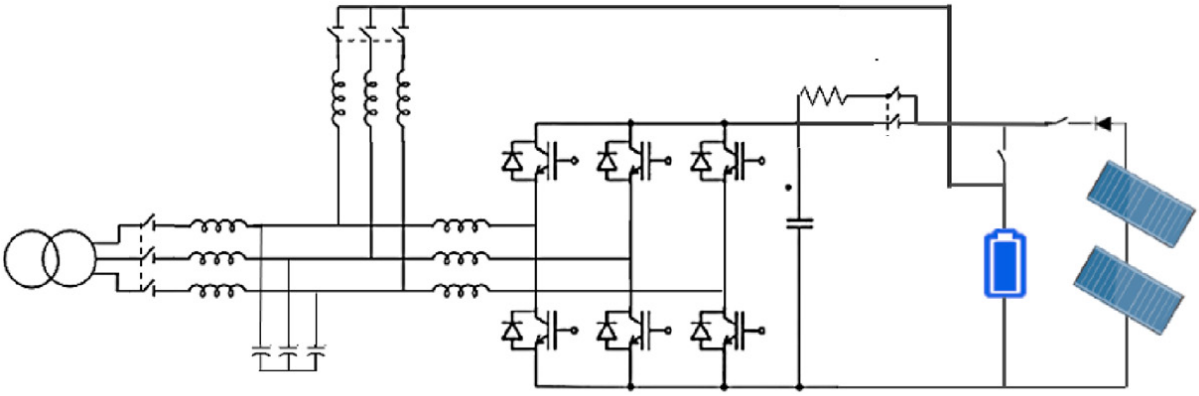

Figure 26 Structure of reconfigurable solar converter

II.3.2.2 Reconfigurable single-input dual-output converter

It is introduced as a single-input dual-output (SIDO) converter to supply DC loads that require high and low voltage levels in domestic micro grid operation (electronic equipment, electric vehicle charging, scooter charging)[18]. Here, a high DC voltage is required for

higher DC loads such as electric vehicle charging, scooter charging, and a low DC voltage is required for smaller DC loads such as electronic equipment. This newly proposed converter has the ability to operate in three different modes by changing its configuration through static switches, depending on the availability of SPV generation and DC load demand.

a) RES DC/DC SIDO mode - two different voltage supplies are provided through solar power generation depending on the DC load demand and solar power availability. As the name of this mode implies two separate outputs are available as buck and boost converter outputs with one input.

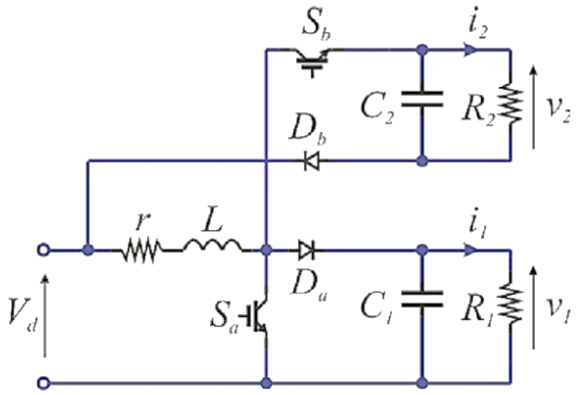

Figure 27 Structure of SIDO at RES DC/DC SIDO mode.

b) Grid/RES double DC output mode - Here, the SIDO converter has been reconfigured into a separate H bridge converter and a buck converter. Here, SPV is connected to smaller DC loads through a buck converter and the grid supplies the large DC loads through an H-bridge converter.

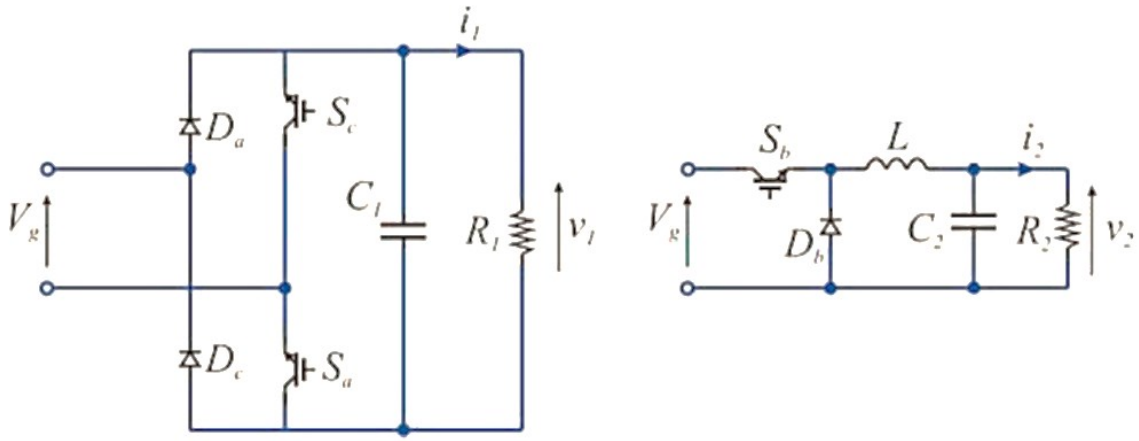

Figure 28 Structure of SIDO at Grid/RES double DC output mode.

c) Grid double DC output mode - SIDO converter reconfigures into a single input double cascade converter by a series connection of an H bridge converter and a buck converter. Static switches are available in this model to feed two-levels of DC loads.

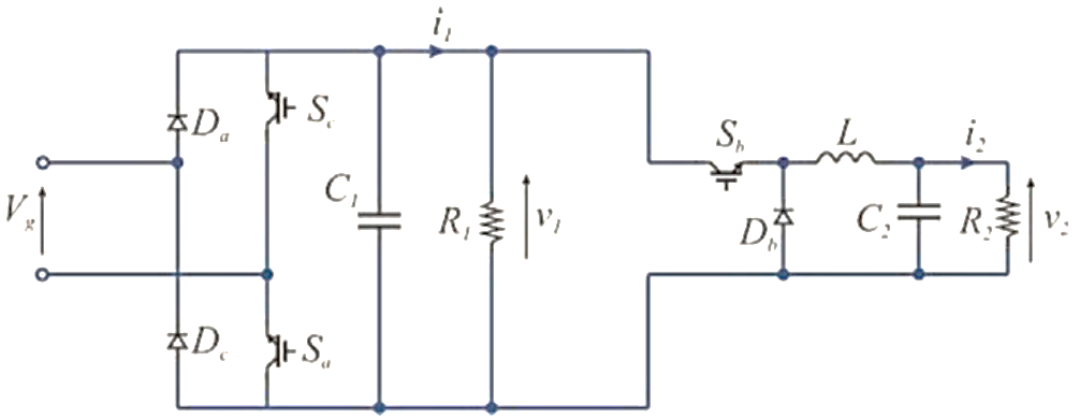

Figure 29 Structure of SIDO at Grid double DC output mode

II.4 Reconfigurable PV system

II.4.1 Quasi-Z-source series resonant DC/DC converter

The main consideration is on MPP tracking of solar panels, under partial shading conditions and different temperatures. Here, the incremental conduction method can be used to calculate the reference input voltage[18].

This converter provides a wide range of input voltage and load regulation capability to the SPVS. The proposed system has the capability to change its configuration into two different configurations as a full-bridge converter or a traditional series resonance converter (SRC) and a single switch qZSSRC as given in Figure and it is operated in following three different modes depending on its point of operation[18].

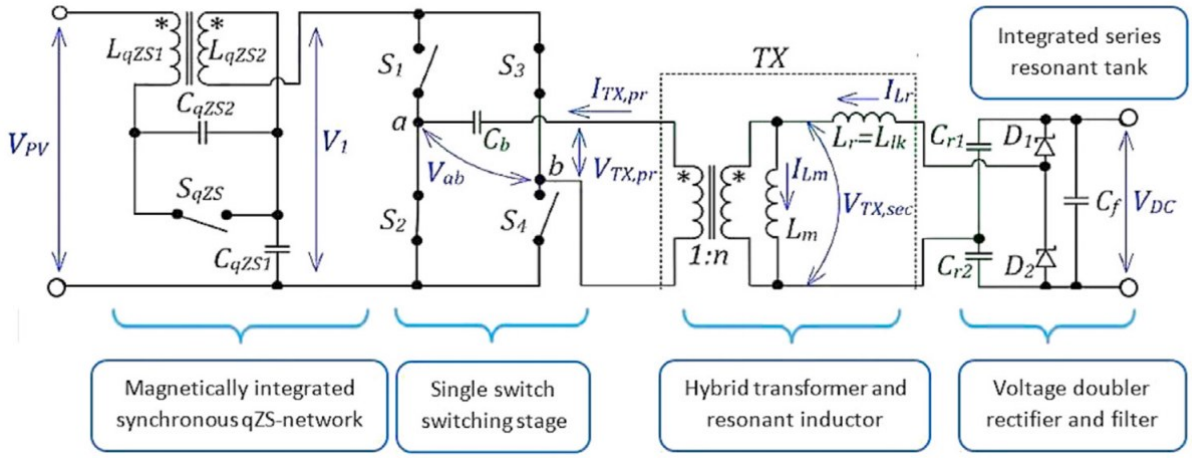

Figure 30 Structure of qZSSRC.

II.4.2 Z-source inverter

ZSI has become an interesting research area related to solar PV inverter performance enhancement in terms of power quality, efficiency and reliability by minimizing the harmonics in the output, introducing fewer power conversion stages and managing converter failures resulted by inevitable shoot-through conditions and capacitor failures respectively. In addition to that, ZSI is used in grid connected and islanded operation of SPVS together with reactive power controlling .As a novel approach, ZSI based MPPT is available for solar power applications[18].

However, the combined operation of grid connected mode and islanded mode while night time reactive power compensation is not proposed for a residential system. Furthermore, solar PV systems based reconfigurable systems will play a major role in future distribution networks[18].

II.4.3 Reconfigurable inductor

Most of the researches are focused on the reconfigurability of the entire converter. There is a low consideration of the reconfigurable operation of a single element of a system. A reconfigurable inductor is proposed as a solution for low-efficiency solar PV boost converters, under low insolation conditions with high current and voltage ripples. This approach can also be used to overcome design limitations on inductor sizing to prevent saturation at high insolation levels[18].

Here, the standard boost converter is modified with three switches and replaced the inductor with a coupling inductor such that it can be reconfigured into two different modes :

•High-L - where, inductors are connected in series to reduce output current and voltage ripple of the solar PV system at low insolation.

•Low-L - where, inductors are connected in parallel. This mode of operation prevents reaching saturation at high insolation levels.

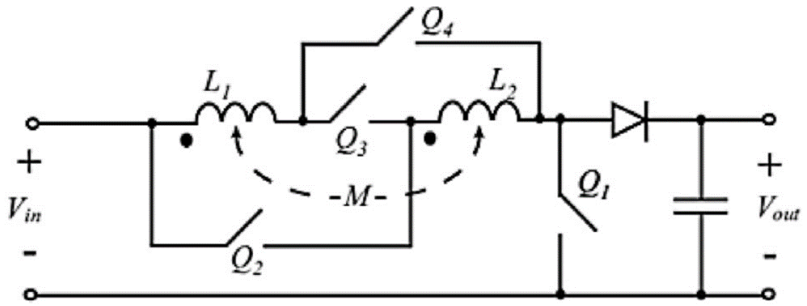

Figure 31 Structure of boost converter with reconfigurable inductor.

II.4.4 Reconfigurable microgrids

The reconfigurability has been introduced for microgrid control architecture as well as for microgrid topology architecture. Most of the researches are based on battery-based inverters for microgrids such that there is a low consideration towards AC generation including wind, hydro and diesel generators. But recently, grid-connected SPV-battery and hydro generation based reconfigurable systems have been proposed. The point of common coupling (PCC) is the common connection point for the grid, the microgrid and the non – linear loads in the system[18].

II.4.5 Reconfigurable architecture

A reconfigurable architecture is proposed for a microgrid consists of distributed generation resources including SPV and power backups. In this study, as control architectures, the conventional centralized, decentralized and hierarchical architectures are under consideration[18].

The main aim of applying reconfigurable concept to the control architecture is to ensure the microgrid operation even there are failures in controllers, data transmission networks, etc. This control architecture consists of four main control layers (local controller (LC), emergency controller, secondary controller and global controller) and an additional control

layer called adversary control (ADVC) layer. Here, the global and secondary layers reside in the master microgrid controller (MMC) while the emergency control layer resides in ADVC, MMC and LC. All controllers are interconnected via the communication layer to operate as a centralized controller[18].

According to the proposed reconfigurable architecture, the microgrid is operated through a decentralized controller. When a failure of LC occurs, the MMC functions as a centralized controller. In an emergency, where both LC and MMC are failed, ADVC functions as a centralized controller. The proposed reconfigurable microgrid can be physically implemented and tested for reconfigurable operation under various operating modes and events.

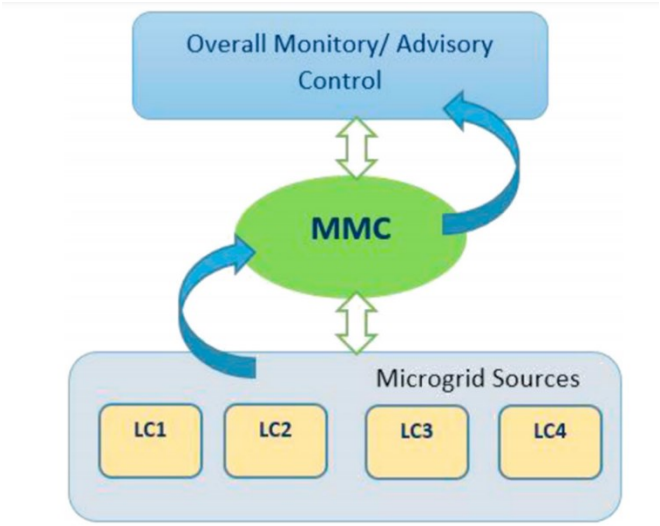

Figure 32 Proposed reconfigurable control architecture.

II.4.6 Reconfigurable distribution networks

With the introduction of distributed generation sources, the distribution network has gained an active nature. High penetration of distributed generation may lead to critical issues related to power reliability, power quality, harmonic levels and protection[18].

A modified boost converter with a reconfigurable inductor is presented for increasing solar energy capture during low light periods.

The radial distribution network of the proposed system is subjected to reconfigurability, focusing on energy costs and the frequency of supply interruptions. This study highlights that to exploit the benefits from the reconfigurable approach, the most appropriate nodes for the microgrid operations under certain conditions should be distinguished. This proposed system

is beneficial to distribution system operators (DSOs) to upgrade their services, exploit new businesses, and hold off investments on modern networks. Microgrid regulators may also find this planning strategy advantageous in terms of profits that can be gained through customer operations and subsides for distribution system advancement.

II.4.7 Reconfigurable distribution networks into microgrids

The main aim of distribution network reconfiguration is to advance the microgrid operation with an economic load dispatch concept considering the uncertainties of the system such as load variations and the cost of SPV, wind generation and battery storage. And also vector regression-based machine learning approaches can forecast such uncertainties in the system[18].

Vaccine-enhanced artificial immune system (Vaccine-AIS) is a suitable multi-modal optimization technique to solve the optimization problem related to this proposed model. The reconfigured network has the capability to adjust its configuration by itself. This approach allows the maximum utilization of renewable energy while reducing the power loss in the distribution network[18].

II.5 Existing types with characteristic

II.5.1 Reconfiguration for TCT topology

The TCT interconnection allows to reduce the overall effects of mismatch. The challenge in a TCT reconfiguration technique consists in connecting PV modules in irradiance-balanced tiers[15][20].

An interesting optimization algorithm based on the use of an equalization index. Irradiance equalization aims to obtain series connected tiers, also called rows, where the sum of the irradiances of the modules is the same. this results in a string where the circulating current is proportional to the given sum of irradiances of one row. The algorithm equalizes the available power on each row, thus an ideal current generator, with the same nominal values, are connected in the string, avoiding mismatch losses[15].

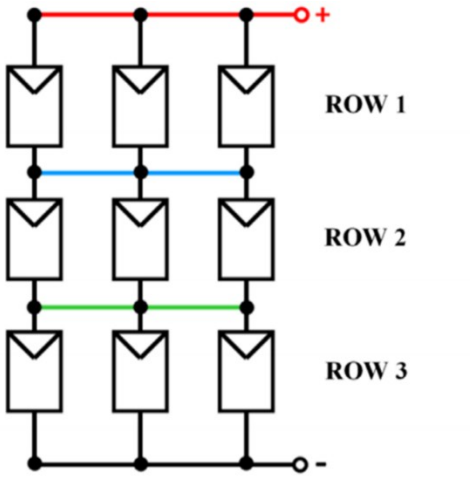

Figure 33 Electrical scheme for a square switching matrix m=n=3.

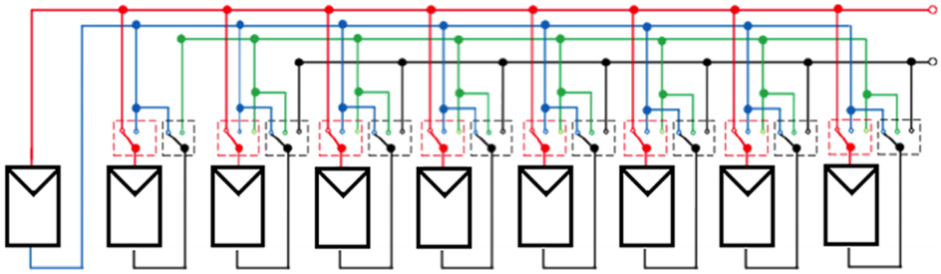

Figure 34 Every module is connected to the electrical bus with m-throw switches

II.5.2 Reconfiguration in SP topology

Reconfiguration by means of SP topology aims to build strings of series-connected modules with similar irradiance levels and then connecting all these strings in parallel. In this way, well irradiated solar panels will not be limited in current by a low irradiance panel of the same string[15].

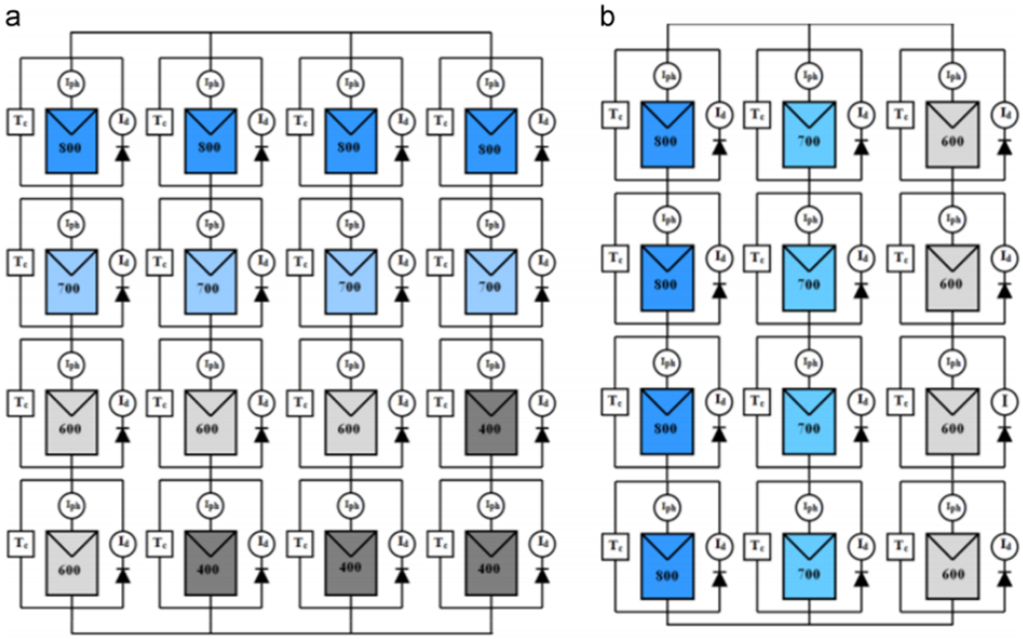

Figure 35 Reconfiguration strategy in SP connection: (a) PV array with four different irradiance levels: 800, 700, 600 and 400 W/m2 , (b) after sorting, PV array is composed by three string with 800, 700 and 600 W/m2 . The PV panels with 400 W/m2 are excluded.

II.6 Fault tolerance

II.6.1 Reconfiguration for Fault Detection and Fault Bypassing

The objective of fault detection is to identify any PV cell faults in the PV panel. Fault bypassing aims at forming a new PV panel configuration to minimize the output power loss caused by PV cell faults. Consider a PV panel assuming a $N \times M$ configuration during normal system operation. For fault detection, we may need to form a PV panel configuration with a selected set of PV cells and measure their combined output power to determine whether a PV cell fault exists in this portion of PV panel. During fault by passing, we may need to form a $K \times M$ PV panel configuration to improve the system output power, where the faulty PV cells, and perhaps some healthy PV cells are excluded from the new configuration $K \leq N$ with a selected set of PV cells and measure their combined output power to determine whether a PV cell fault exists in this portion of PV panel. During fault bypassing, we may need to form a $Nopt \times Mopt$ PV panel configuration to improve the system output power, where the faulty PV cells, and perhaps some healthy PV cells are excluded from the new configuration ($Nopt \times Mopt < N \times M$)[21][22][23].

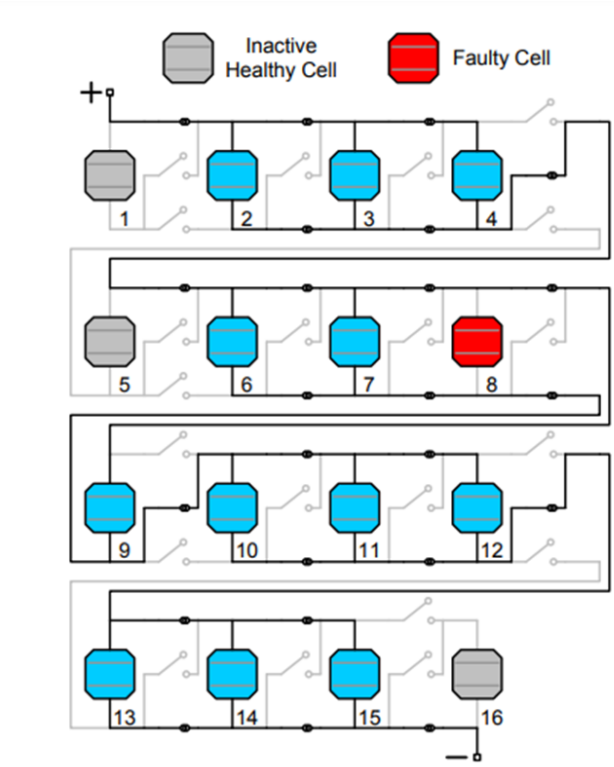

Figure 36 Example of PV panel reconfiguration during fault detection and bypassing.

II.6.2 Fault Detection Algorithm

The basic step of the fault detection algorithm is the Fault Existence, checking algorithm, which determines whether a PV cell fault exists in a set of $K \times M$ PV cells. We track the maximum output power of the $K \times M$ PV panel configuration using the charger in the PV system at Step 3 of the Fault Existence Checking algorithm. In reality must be larger than or equal to a threshold value K_{min} such that the output voltage of the $K \times M$ PV panel configuration is high enough to properly drive the charger. This means that the Fault Existence Checking algorithm cannot run on a PV panel configuration smaller than $Kmin \times M$ [21][24].

The fault detection algorithm has two steps:

a) First step : determine which row the faulty PV cell is located at (row search);

b) Second step : determine which column the faulty PV cell is located at (column earch).

To find the location of the potential faulty PV cell in the $K \times M$ PV panel, we first run the Fault Existence Checking algorithm on the whole PV panel. If it is confirmed that no PV

cell fault exists, the fault detection algorithm will terminate. Otherwise, the fault detection algorithm will continue to find the location of the PV cell fault as explained next[21][22].

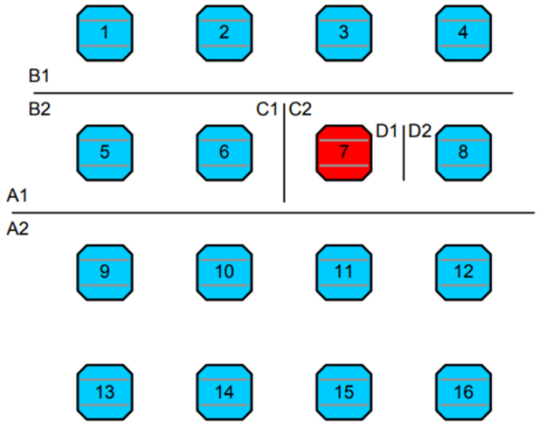

Figure 37 Demonstration of the fault detection algorithm.

We use Figure 33 to demonstrate how the row search and column search proceed. In this example, $N = 4$, $K = 2$ and $Kmin = 2$. For row search, we bisect the PV panel into the first two rows ($A1$) and the remaining two rows ($A2$). We run the Fault Existence Checking algorithm on $A1$ and find out that $A1$ contains a faulty PV cell. Then we bisect $A1$ into the first row ($B1$) and the second row ($B2$). The size of $B1$ is smaller than $Kmin \times M$. Therefore, we form a $Kmin \times M$ (2×4) configuration from $B1$ along with the third row, which has been confirmed to contain only healthy PV cells, and subsequently, run the Fault Existence Checking algorithm on this configuration. We determine that $B1$ does not contain the faulty PV cell, and therefore, the faulty PV cell is within $B2$. Now we have located the row containing the faulty PV cell[22][21].

For column search, we bisect $B2$ into PV cells 5 and 6 ($C1$) and PV cells 7 and 8 ($C2$). We run the Fault Existence Checking algorithm on $C1$ along with PV cells 3, 4, 9 ~ 12 that are confirmed healthy. We pick these healthy PV cells, because in this way we can form a configuration, with PV cells 7 and 8 bypassed between the first PV cell group (PV cells 3 ~ 6) and the second PV cell group (PV cells 9 ~ 12). We find out that $C1$ does not contain the faulty PV cell, and therefore, $C2$ contains the faulty PV cell. We bisect $C2$ into PV cell 7 ($D1$) and PV cell 8 ($D2$). We form a configuration from $D1$ along with PV cells 4 ~ 6 and 9 ~ 12, and run the Fault Existence Checking algorithm on this configuration. We confirm that the faulty PV cell is PV cell 7, and thereby, conclude the column search[21].

II.6.3 Fault Bypassing Algorithm

The fault bypassing algorithm determines the optimal configuration of a PV panel, such that the PV system output power loss due to PV cell faults is minimized. We need to decide (i) the number of active healthy PV cells S, and (ii) the optimal PV panel configuration $Nopt \times Mopt(= s)$ [22].

Let us denote the number of factors of by F(S).The maximum output power of a PV panel is approximately proportional to S. And a S value is preferred if F(S)is larger, since we have more choices of PV panel configurations with this S value[21].

Assume that the PV panel has $N \times M$ PV cells and PV cell faults have been identified so far. Therefore, we have $Smax = N \times M - L$. First, we determine a set of candidate S values in ascending order, which satisfies $S + F(S) \geq Smax + F(Smax)$ .There are F(S) possible configurations using S active healthy PV cells. Among these configurations, there exists an optimal configuration that provides maximum PV system output power Pmax(s). Based on the PV cell and charger model, we find the optimal Sopt value by ternary search on the set of Candidate S values, such that Pmax(Sopt) is the maximum achievable PV system output power. The optimal PV panel configuration is determined accordingly[21][22].

Figure 38 Computer-controlled programmable switch board.

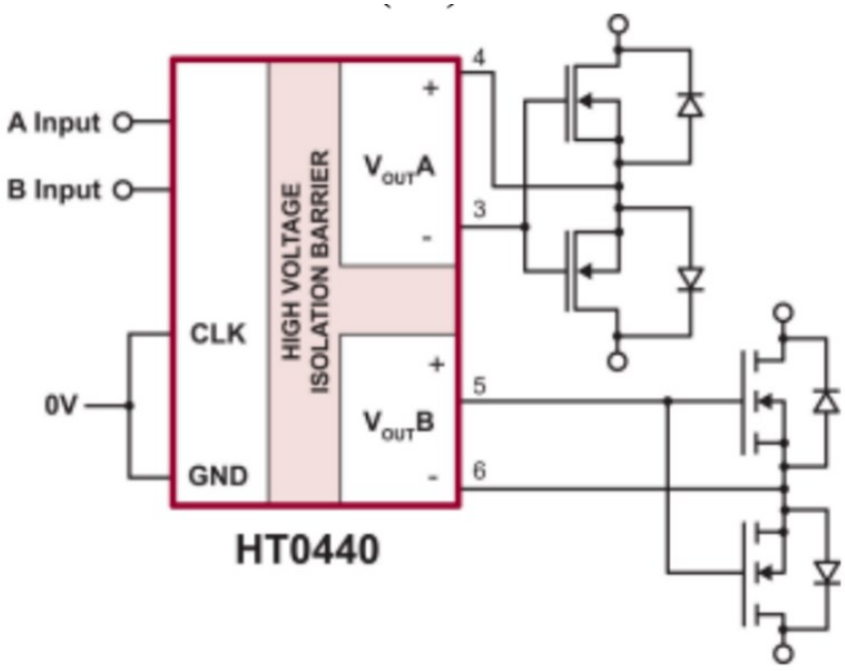

Figure 39 Semiconductor realization of the switches.

II.6.4 Prototype of the fault-tolerant PV system

Implemented to substantiate the feasibility and effectiveness of our structure design and control algorithms. Figure shows the prototype of the reconfigurable PV panel. The PV panel consists of 16 PV cells, each of which (except for the last PV cell) is integrated with three toggle switches. PV cells and toggle switches are mounted on top of an acrylic board, whereas connection wires are routed in the back of the board[21].

A PV cell fault can be emulated by blocking the surface of a PV cell, since zero solar irradiance on a PV cell results in zero output current, which is equivalent to a PV cell fault[22].

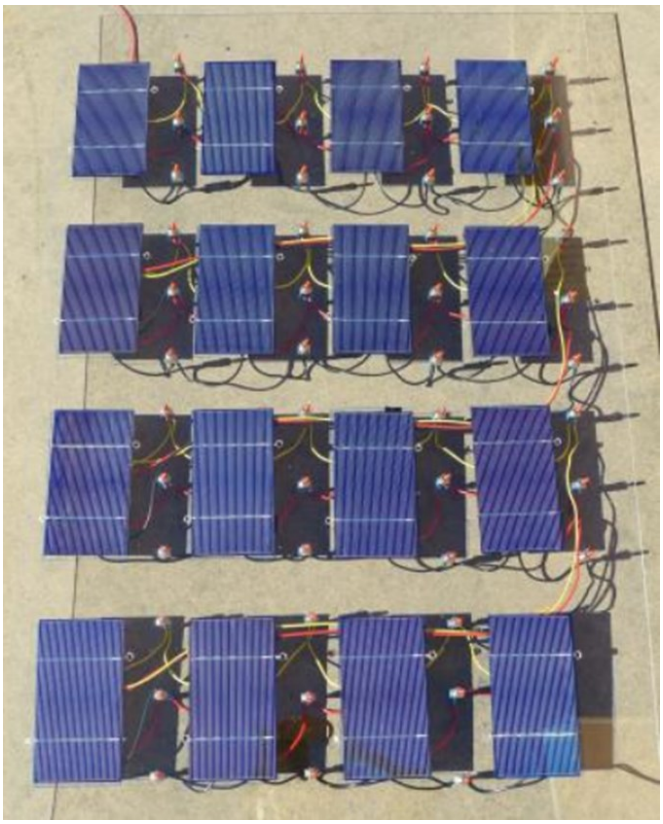

Figure 40 Prototype of the fault-tolerant PV system.

II.7 Conclusion

Along this chapter we presented reconfigurable PV generators and their benefits, and we explained the difference between the configuration and the reconfiguration by clarifying the concept of each of item and their objectives in PV systems optimization and diagnosis.

Chapter III
Dynamic and static simulation under different shading conditions

III.1 Introduction

The photovoltaic generator faces several problems, perhaps the most famous of which is shading, which affects its production capacity greatly and reduces its performance and efficiency. Problems are decupled when a large-scale PV generator are used. To improve such systems, we propose in this study to adapt dynamically the topology of the PV generator to the actual situation of the system.

In this chapter, we will present another research approach, in contrast to the classical approach. First, we will present different models and different scenarios to be used for system test and evaluation. For dynamic optimization an algorithm is proposed to estimate and apply the most favorable reconfigurable topologies. When there is a fault or shadowing, the topology is immediately changed to meet the system requirements and reach the maximum value of the power.

III.2 Simulation model presentation

In this work, we propose the architecture of the system as presented in figure 41. The layout configuration consists of 20 PV modules assembled into five and four columns. In each row four PV modules are connected in parallel. The voltage across each row is same as open-circuit voltage of a single PV module. The module is a Yingli Energy YL245P-29P, this module comprises 60 cells and draw 250 watts in STC conditions. The I-V and P-V characteristics of the module are given in the figure 42.

The main configuration is based in TCT scheme, and the connection between each column is replaced by controlled switch. For this example, we need 12 switches which require a reasonable extra cost for the PV installation. Switches must have low conduction losses and operate at high frequencies with a very short switching time.

This configuration allows to have a total power of 4900 Watts with a short-circuit current equal to 34.5 A and an open-circuit time of 189 Volts

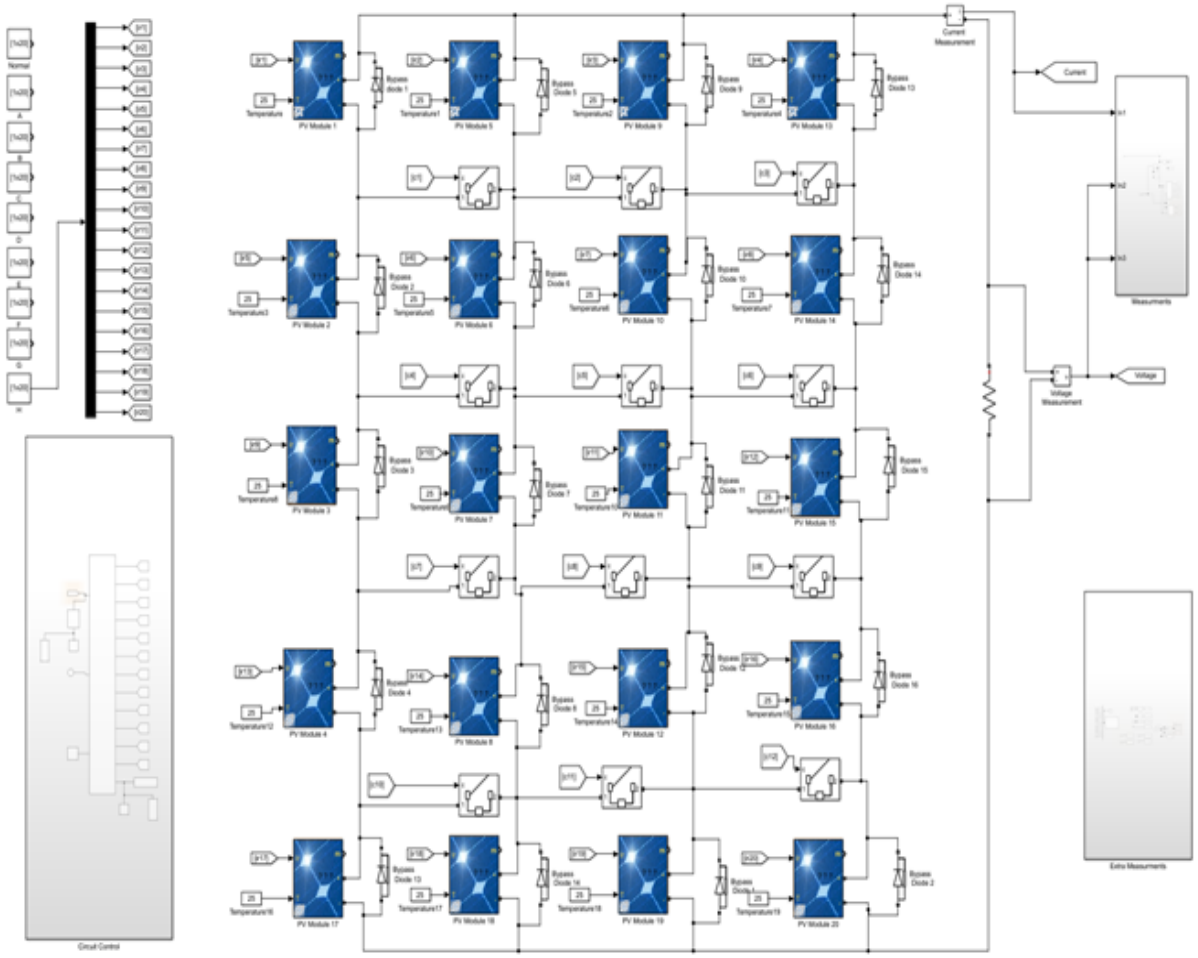

Figure 41 Simulation Model under Simulink environment

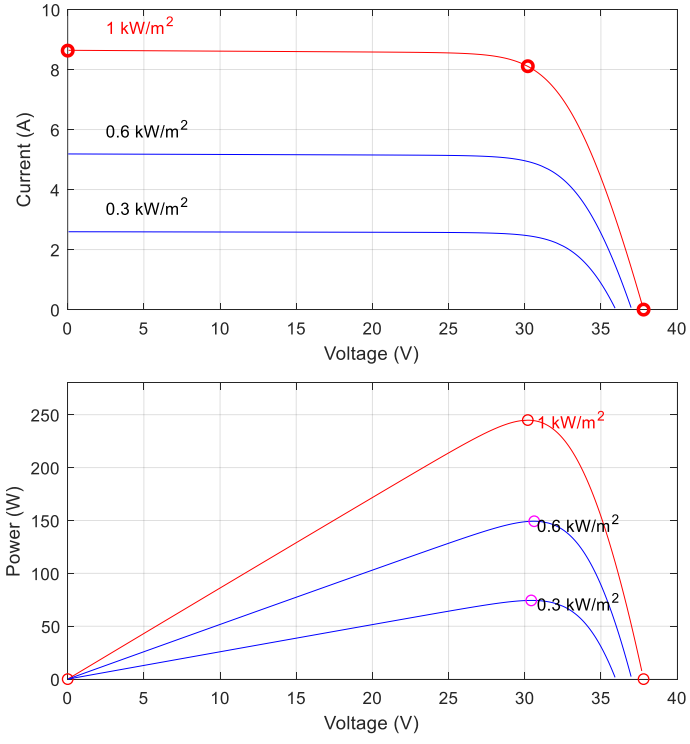

Figure 42 I-V and P-V characteristic of the YL245P-29P module

III.3 Shading scenarios

The PV array performance is mostly influenced by different shading conditions and patterns[25][26], and for that we created some realistic scenarios for different partial shading experiences. We generate 8 different scenarios to analysis maximum data from simulation.

Table 3 Reference Scenario

1000 W/m²	1000 W/m²	1000 W/m²	1000 W/m²
1000 W/m²	1000 W/m²	1000 W/m²	1000 W/m²
1000 W/m²	1000 W/m²	1000 W/m²	1000 W/m²
1000 W/m²	1000 W/m²	1000 W/m²	1000 W/m²
1000 W/m²	1000 W/m²	1000 W/m²	1000 W/m²

However, we have to obtain a reference I-V and P-V characteristics for the PV generator, for that raison we execute the simulation with perfect climatic conditions: $Ir = 1000\ W/m^2$ and $T = 25\ C^{\circ}$. We use tables as above to have a spatial representation of each scenario, which help to visualize the irradiance covering.

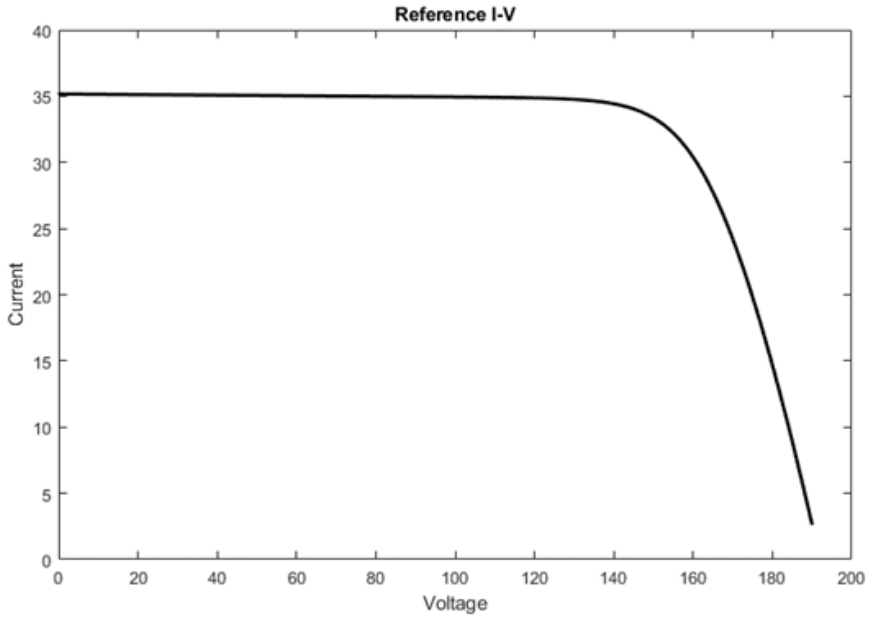

Figure 43 I-V Curve under reference conditions

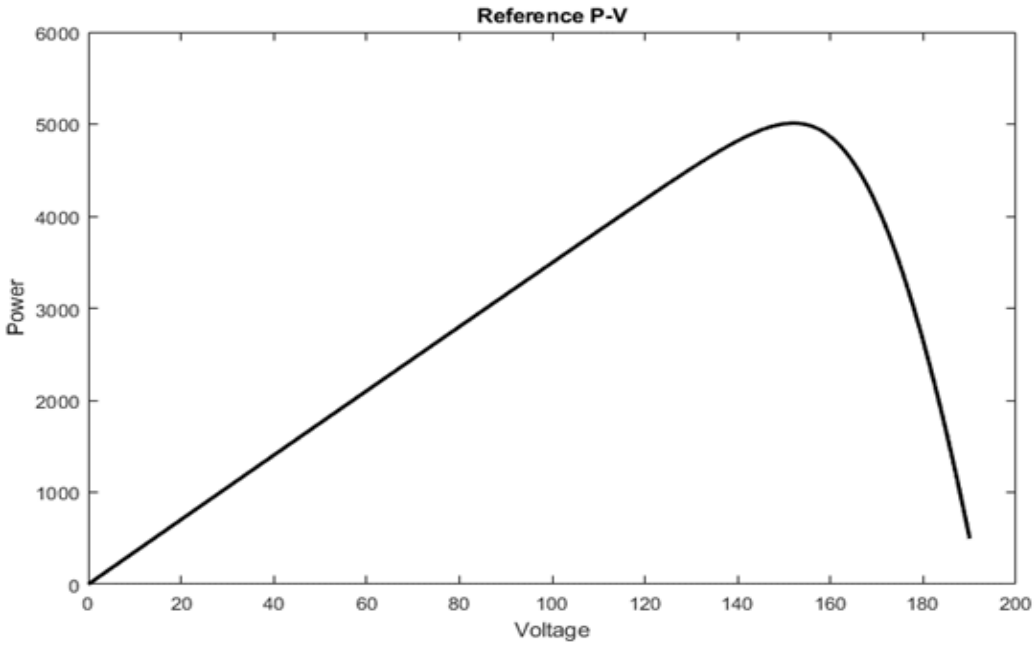

Figure 44 P-V Curve under reference condition

III.3.1 Corner shading

Table 4 (A) Corner shading scenario

1000 W/m²	1000 W/m²	1000 W/m²	1000 W/m²
1000 W/m²	1000 W/m²	1000 W/m²	1000 W/m²
1000 W/m²	1000 W/m²	800 W/m²	800 W/m²
1000 W/m²	1000 W/m²	500 W/m²	500 W/m²
1000 W/m²	1000 W/m²	200 W/m²	200 W/m²

Under this shading pattern, the left corner positioned modules in a 5 × 4 PV array are subjected to distinct insolation levels, termed as corner shading:

- PV11 PV12 are shaded at 800 W/m²
- PV15 PV16 are shaded at 500 W/m²
- PC19 PV20 are shaded at 200 W/m²

The remaining modules are shaded at 1000 W/m² respectively.

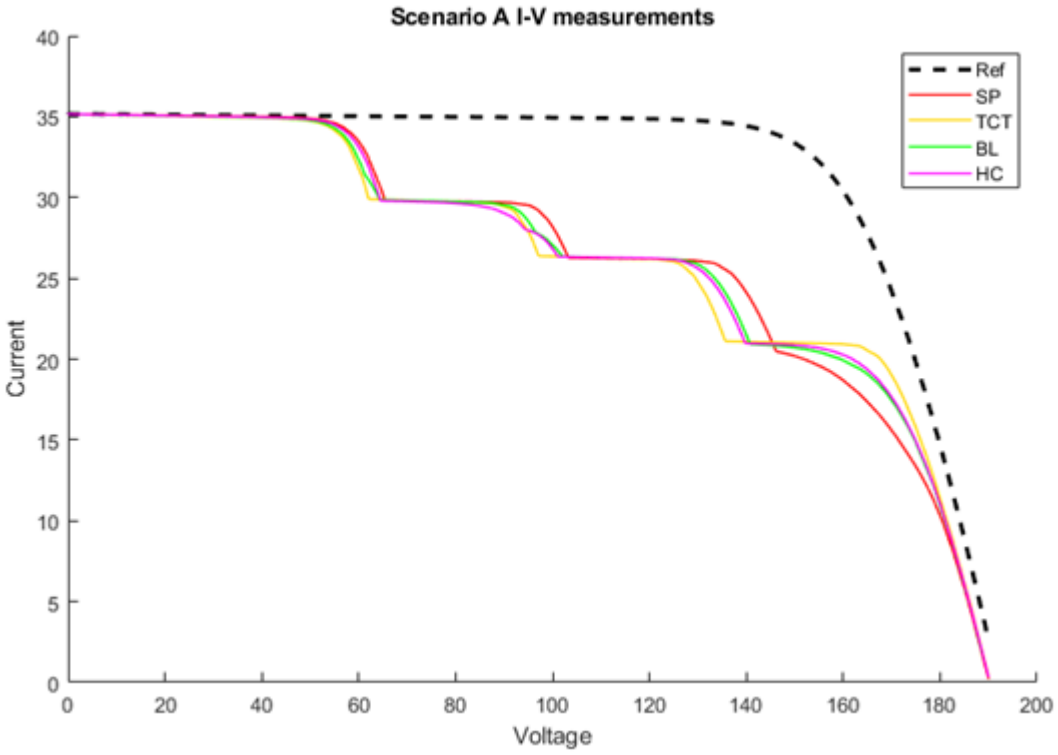

Figure 45 I-V Curve under corner shading condition

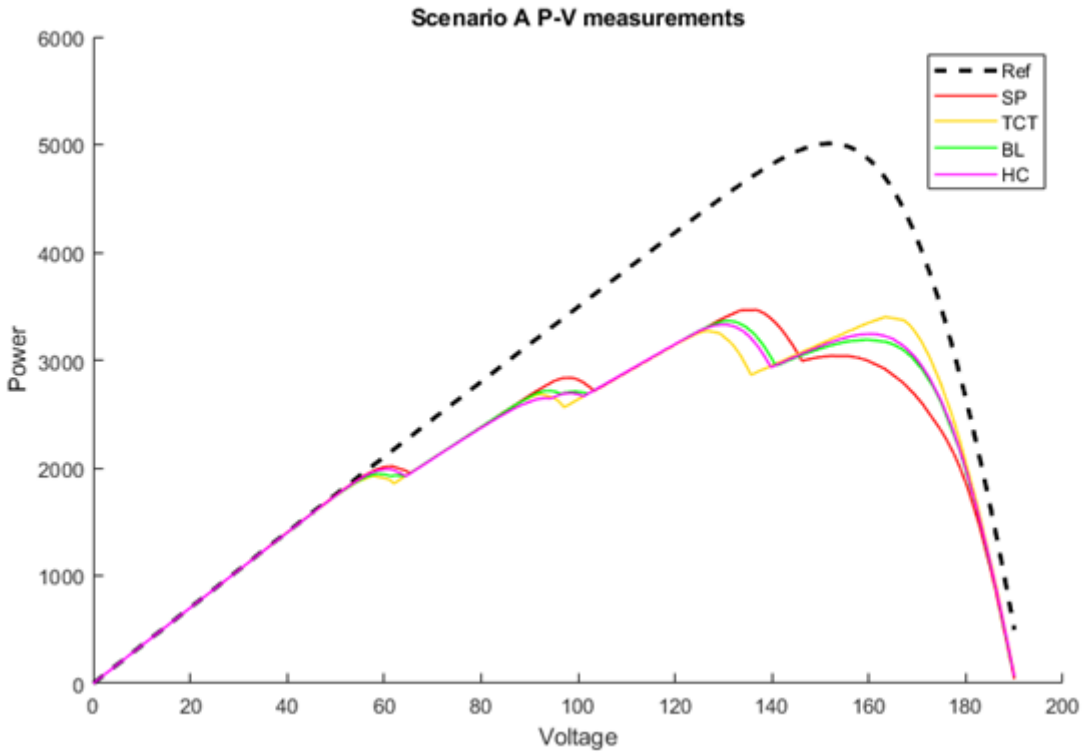

Figure 46 P-V Curve under corner shading condition

III.3.2 Center shading

Table 5 (B) Center shading scenario

1000 W/m²	1000 W/m²	1000 W/m²	1000 W/m²
700 W/m²	700 W/m²	700 W/m²	700 W/m²
200 W/m²	350 W/m²	550 W/m²	800 W/m²
700 W/m²	700 W/m²	700 W/m²	700 W/m²
1000 W/m²	1000 W/m²	1000 W/m²	1000 W/m²

Under this shading pattern, the modules which are positioned at the right side in the array are subjected to distinct levels of insolation, the shaded modules are:

- PV12 are shaded at 800 W/m²
- PV5 PV6 PV7 PV8 PV13 PV14 PV15 PV16 are shaded at 700 W/m²
- PV9 are shaded at 200 W/m²
- PV10 are shaded at 350 W/m²
- PV11 are shaded at 550 W/m²

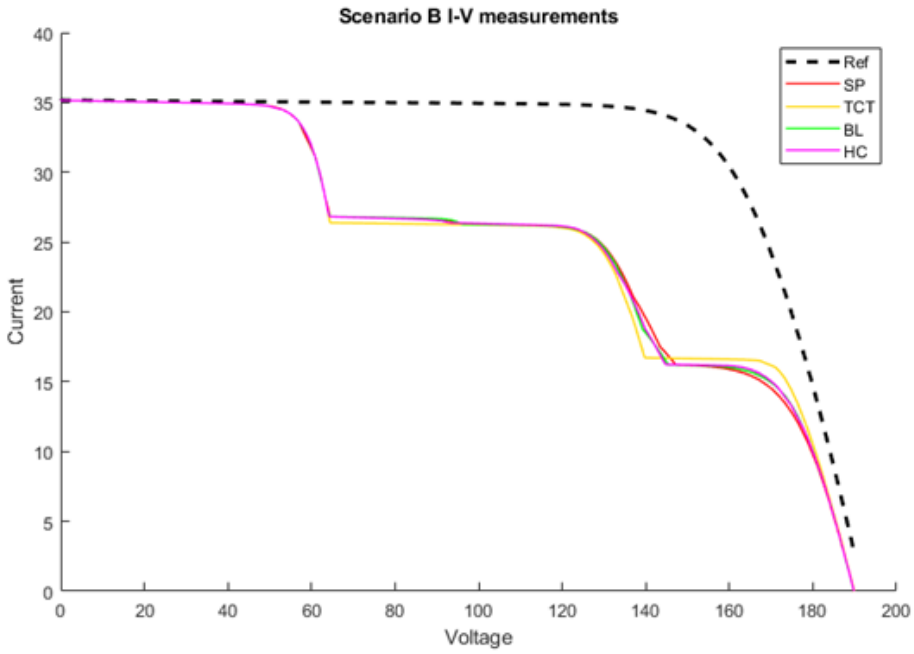

Figure 47 I-V Curve under center shading condition

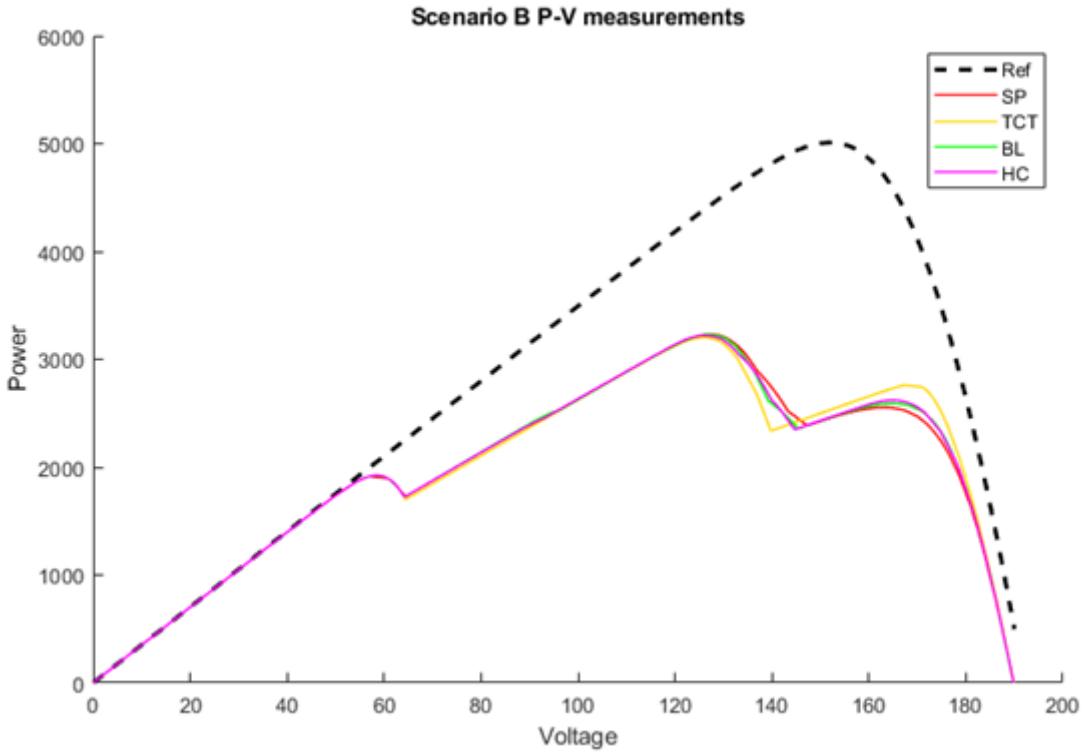

Figure 48 P-V Curve under center shading condition

III.3.3 Right side shading

Table 6 (C) Right side shading scenario

800 W/m²	600 W/m²	350 W/m²	200 W/m²
800 W/m²	600 W/m²	350 W/m²	200 W/m²
1000 W/m²	1000 W/m²	1000 W/m²	1000 W/m²
1000 W/m²	1000 W/m²	1000 W/m²	1000 W/m²
1000 W/m²	1000 W/m²	1000 W/m²	1000 W/m²

Under this shading pattern, the modules which are positioned at the right side in the array are subjected to distinct levels of insolation, the shaded modules are:

- PV1 PV5 are shaded at 800 W/m²
- PV2 PV6 are shaded at 600 W/m²

- PV3 PV7 are shaded at 350 W/m²
- PV4 PV8 are shaded at 200 W/m²

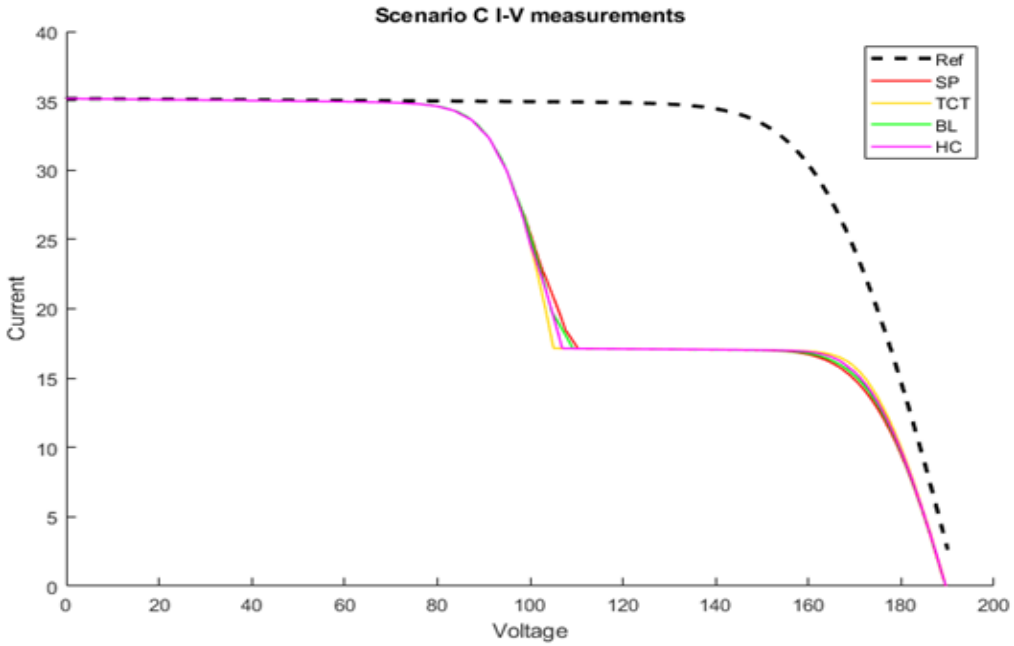

Figure 49 I-V Curve under right side shading condition

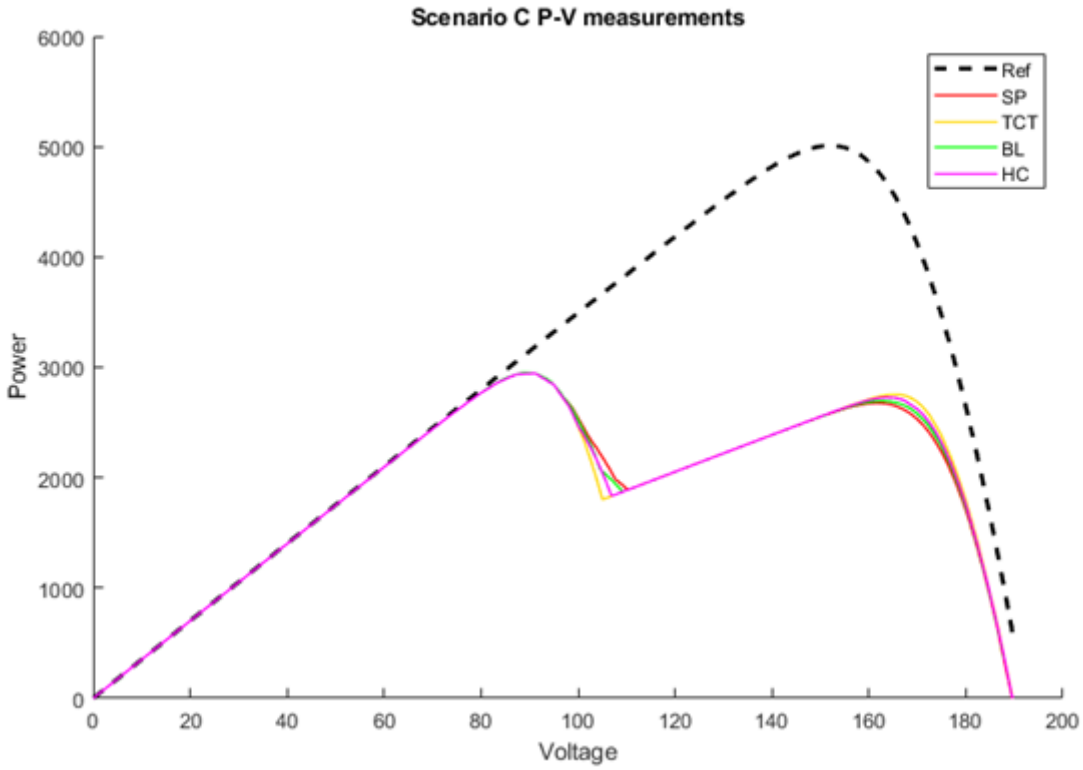

Figure 50 P-V Curve under right side condition

III.3.4 Bottom side end shading

Table 7 (D) Bottom side end shading scenario

800 W/m²	1000 W/m²	1000 W/m²	1000 W/m²
650 W/m²	1000 W/m²	1000 W/m²	1000 W/m²
500 W/m²	1000 W/m²	1000 W/m²	1000 W/m²
350 W/m²	1000 W/m²	1000 W/m²	1000 W/m²
200 W/m²	1000 W/m²	1000 W/m²	1000 W/m²

Under this shading pattern, the bottom side end positioned modules in a 5 × 4 PV array are subjected to distinct insolation levels, termed as bottom side end shading, the shaded modules are:

- PV1 are shaded at 800 W/m²
- PV5 are shaded at 650 W/m²
- PV9 are shaded at 500 W/m²
- PV13 are shaded at 350 W/m²
- PV17 are shaded at 200 W/m²

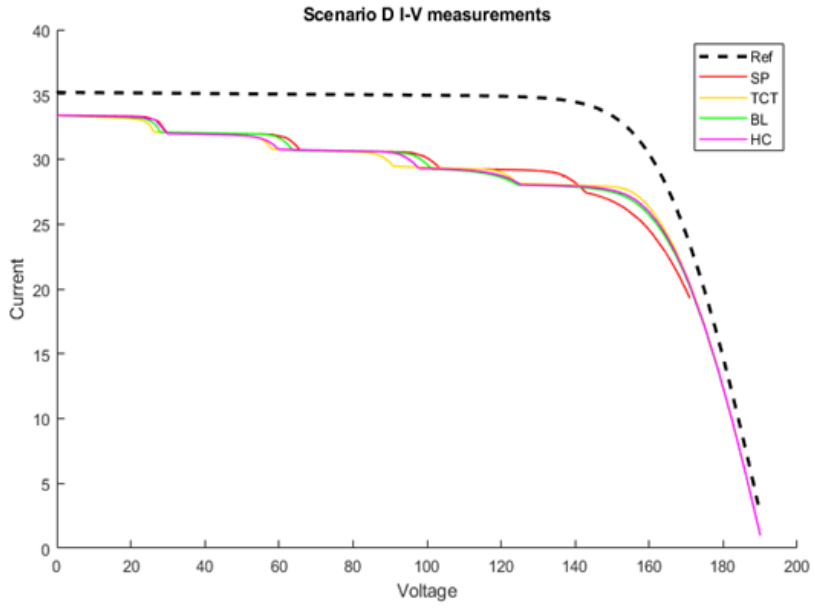

Figure 51 I-V Curve under bottom side end condition

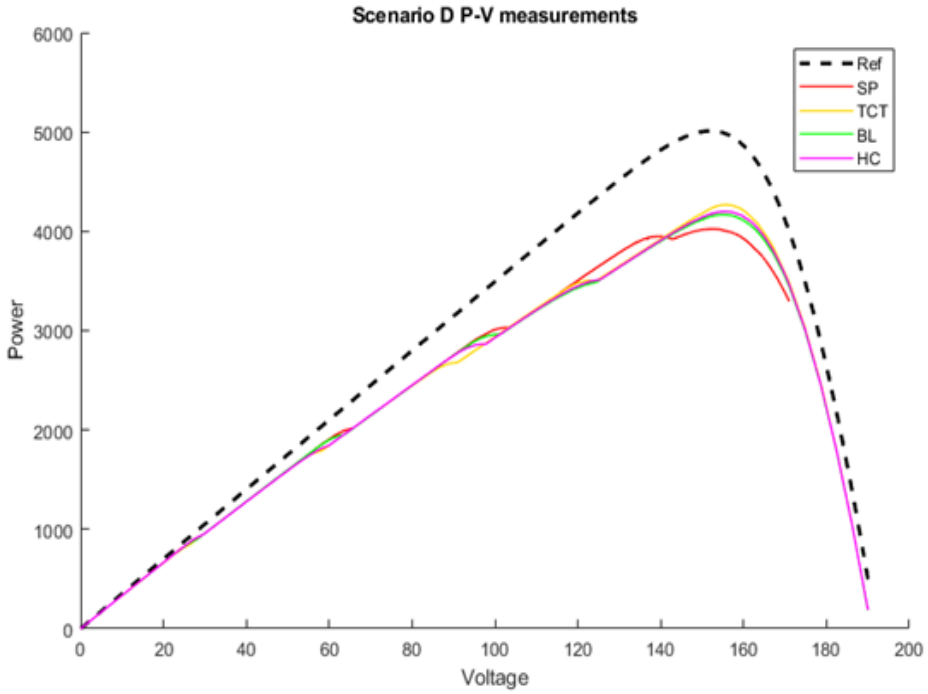

Figure 52 P-V Curve under bottom side end condition

III.3.5 L-shape shading

Table 8 (E) L-shape shading scenario

800 W/m²	600 W/m²	400 W/m²	200 W/m²
600 W/m²	1000 W/m²	1000 W/m²	1000 W/m²
500 W/m²	1000 W/m²	1000 W/m²	1000 W/m²
350 W/m²	1000 W/m²	1000 W/m²	1000 W/m²
200 W/m²	1000 W/m²	1000 W/m²	1000 W/m²

Under this shading pattern, the L-shaped positioned modules in a 5 × 4 PV array are subjected to distinct insolation levels, termed as L-shape shading, The shaded modules are:

- PV1 are shaded at 800 W/m²
- PV2 PV5 are shaded at 600 W/m²
- PV3 are shaded at 400 W/m²

- PV4 PV17 are shaded at 200 W/m²
- PV13 are shaded at 350 W/m²

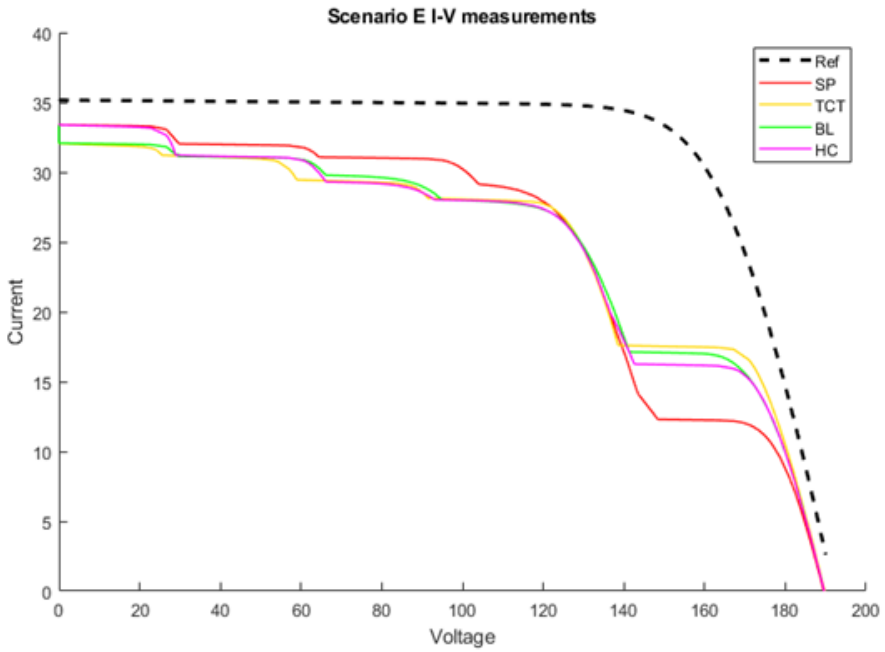

Figure 53 I-V Curve under L-shape condition

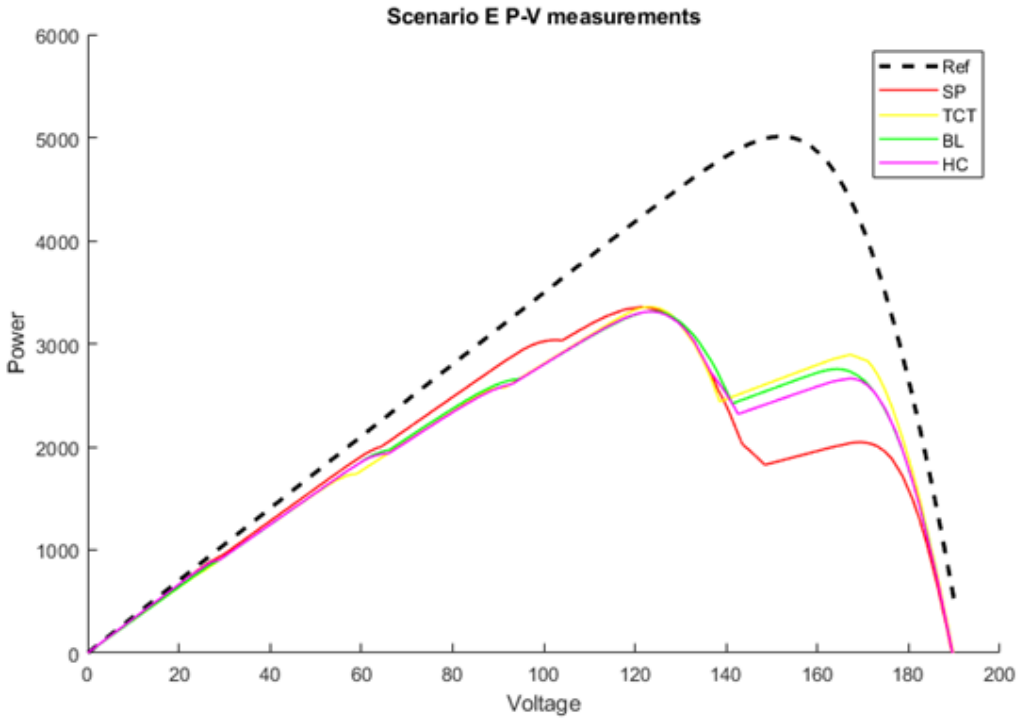

Figure 54 P-V Curve under L-shape condition

III.3.6 Frame shading

200 W/m²	350 W/m²	600 W/m²	800 W/m²
350 W/m²	1000 W/m²	1000 W/m²	1000 W/m²
500 W/m²	1000 W/m²	1000 W/m²	1000 W/m²
650 W/m²	1000 W/m²	1000 W/m²	1000 W/m²
800 W/m²	1000 W/m²	1000 W/m²	1000 W/m²

Table 9 (E) Frame shading scenario

Under this shading pattern, the frame shape positioned modules in a 5 × 4 PV array are subjected to distinct insolation levels, termed as frame shape shading, the shaded modules are:

- PV1 are shaded at 200 W/m²
- PV9 are shaded at 500 W/m²
- PV2 PV5 are shaded at 350 W/m²
- PV3 PV13 are shaded at 600 W/m² and 650 W/m² respectively
- PV4 PV17 are shaded at 800 W/m²

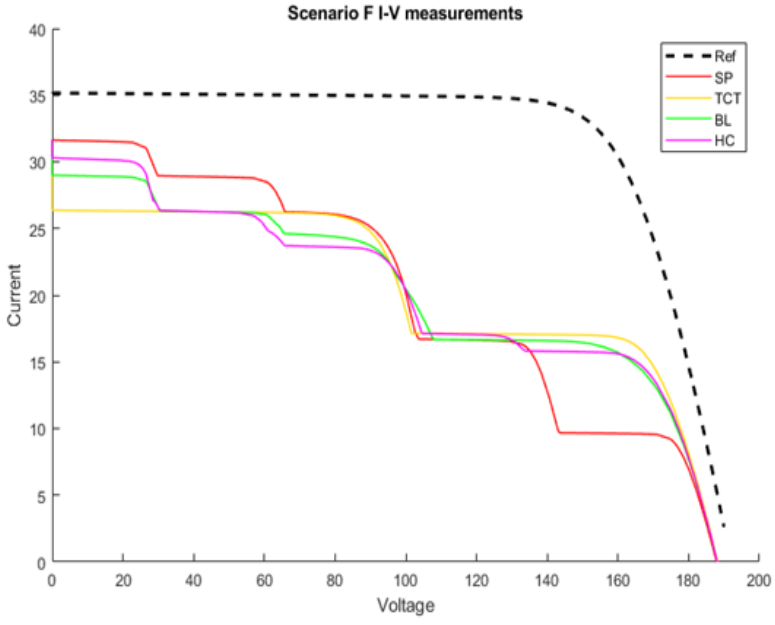

Figure 55 I-V Curve under Frame condition

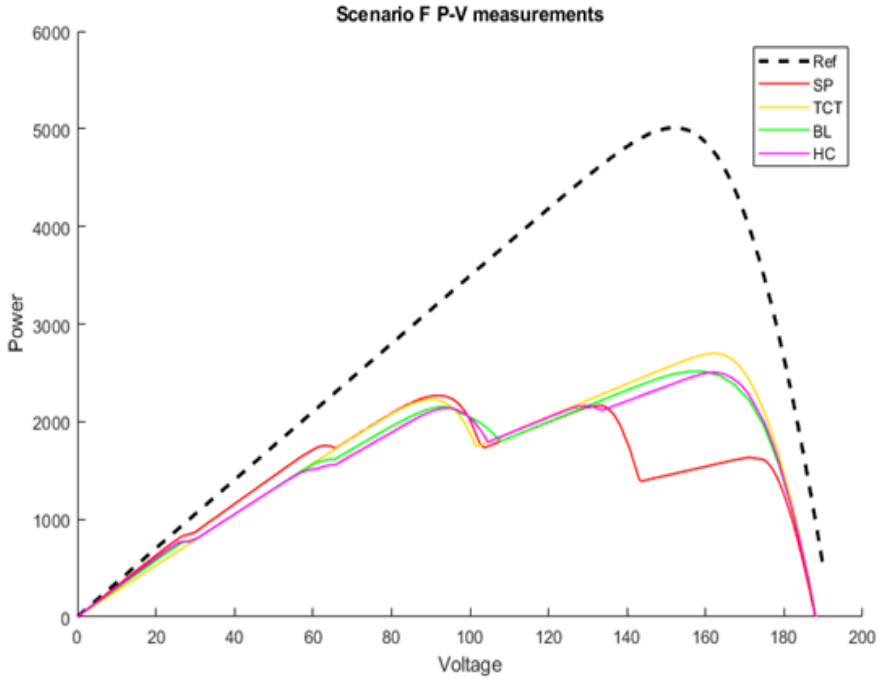

Figure 56 P-V Curve under Frame condition

III.3.7 Random shading

Table 10 (G) Random shading scenario

200 W/m²	1000 W/m²	600 W/m²	1000 W/m²
800 W/m²	1000 W/m²	1000 W/m²	350 W/m²
200 W/m²	1000 W/m²	1000 W/m²	1000 W/m²
350 W/m²	650 W/m²	350 W/m²	600 W/m²
200 W/m²	350 W/m²	1000 W/m²	1000 W/m²

Under this shading pattern, the modules are shaded in random manner with distinct insolation levels, termed as random shading, the shaded modules are:

- PV1 PV4 PV7 PV9 PV12 PV17 PV19 PV20 are shaded at 200 W/m²
- PV3 PV14 PV16 are shaded at 600 and 650 W/m²
- PV5 are shaded at 800 W/m²

- PV8 PV13 PV15 PV18 are shaded at 350 W/m²

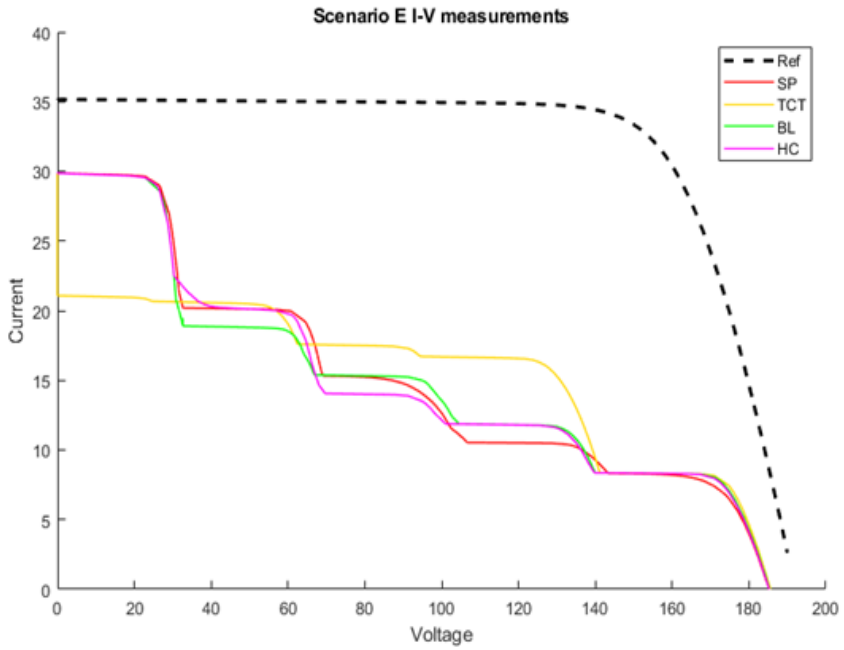

Figure 57 I-V Curve under Random condition

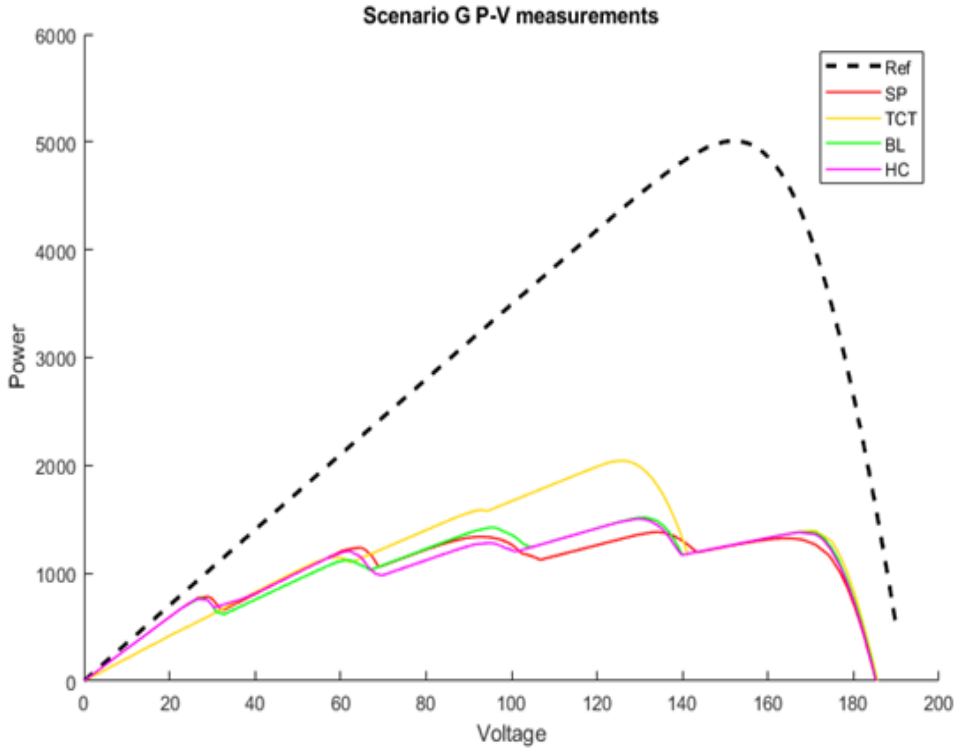

Figure 58 P-V Curve under Random condition

III.3.8 Diagonal shading

Table 11 (H) Diagonal shading scenario

800 W/m²	1000 W/m²	1000 W/m²	1000 W/m²
800 W/m²	600 W/m²	1000 W/m²	1000 W/m²
1000 W/m²	600 W/m²	350 W/m²	1000 W/m²
1000 W/m²	1000 W/m²	350 W/m²	200 W/m²
1000 W/m²	1000 W/m²	1000 W/m²	200 W/m²

Under this pattern, the shading of the modules in the array is diagonal fashion with distinct levels of insolation, termed as diagonal, the shaded modules are:

- PV1 PV5 are shaded at 800 W/m²
- PV6 PV10 are shaded at 600 W/m²
- PV11 PV15 are shaded at 350 W/m²
- PV16 PV20 are shaded at 200 W/m²

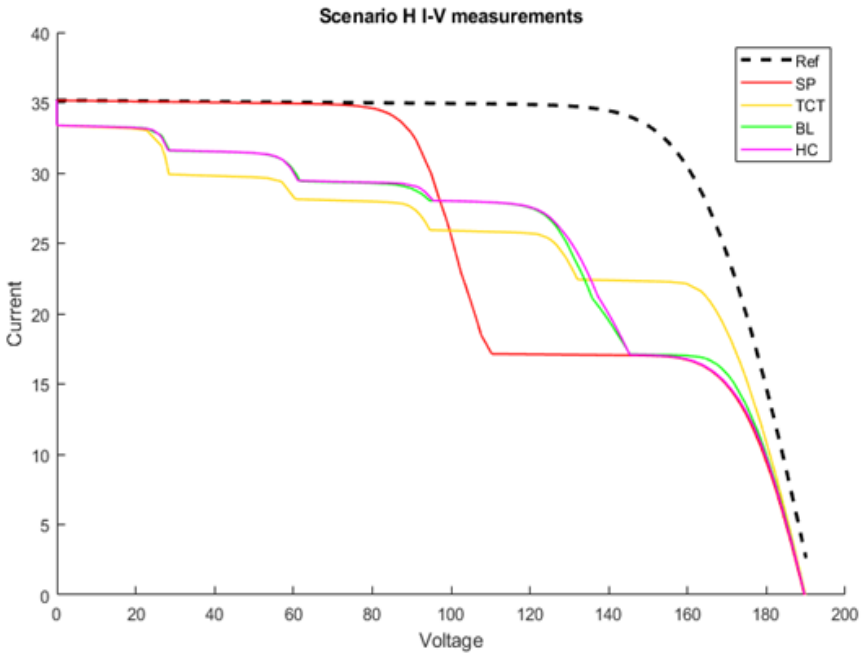

Figure 59 I-V Curve under Diagonal shading condition

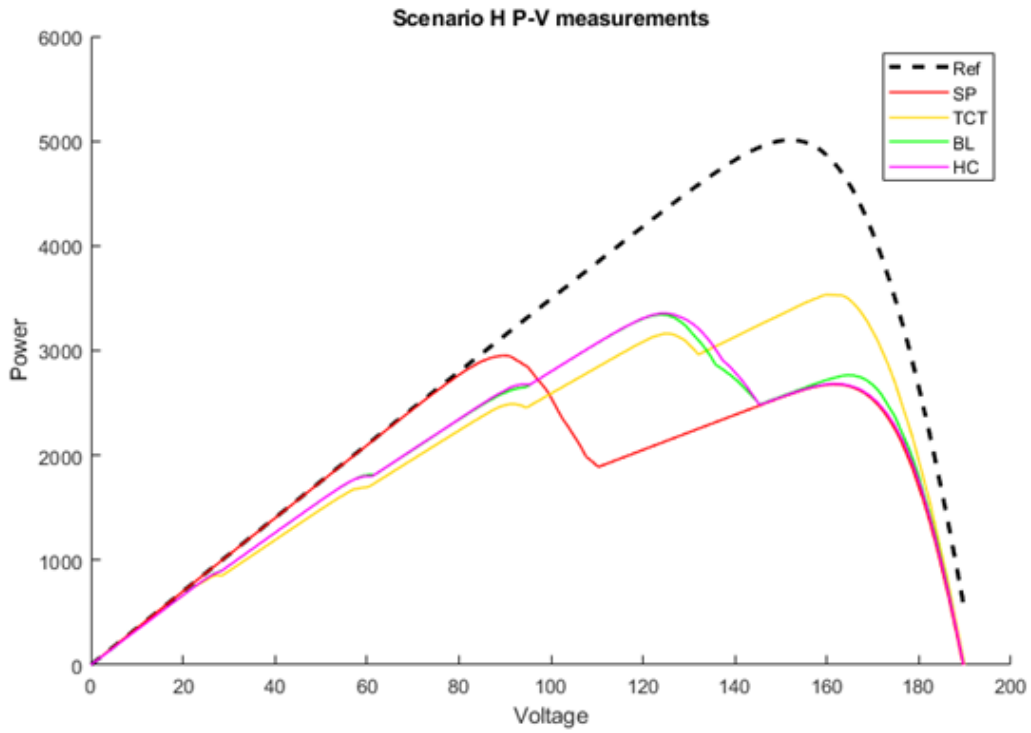

Figure 60 P-V Curve under Diagonal shading condition

III.4 Comparing the different PV array configurations

The PV array configurations such as SP, TCT, HC and BL are compared in this section to study their performance under various partial shading conditions. The main factors considered to analyze the performance of PV configurations are Maximum power point (MPP), Power losses, and Fill factor.

III.4.1 Power losses (LOSS%)

It is the difference in MMP during uniform insolation to partial shading conditions and it is expressed in percentage. The power loss can be calculated by the equation above:

$$LOSS\ (\%) = \frac{MPP_U - MPP_S}{MPP_U} \times 100$$

Where:

MPP_U: Maximum power point under uniform (perfect) conditions

MPP_S: Maximum power point under different partial shading conditions

In the figure 61, we illustrate the power loss for the different configurations under the overmentioned scenarios. We note that the TCT configuration is the one that have the lesser power loss in almost scenarios.

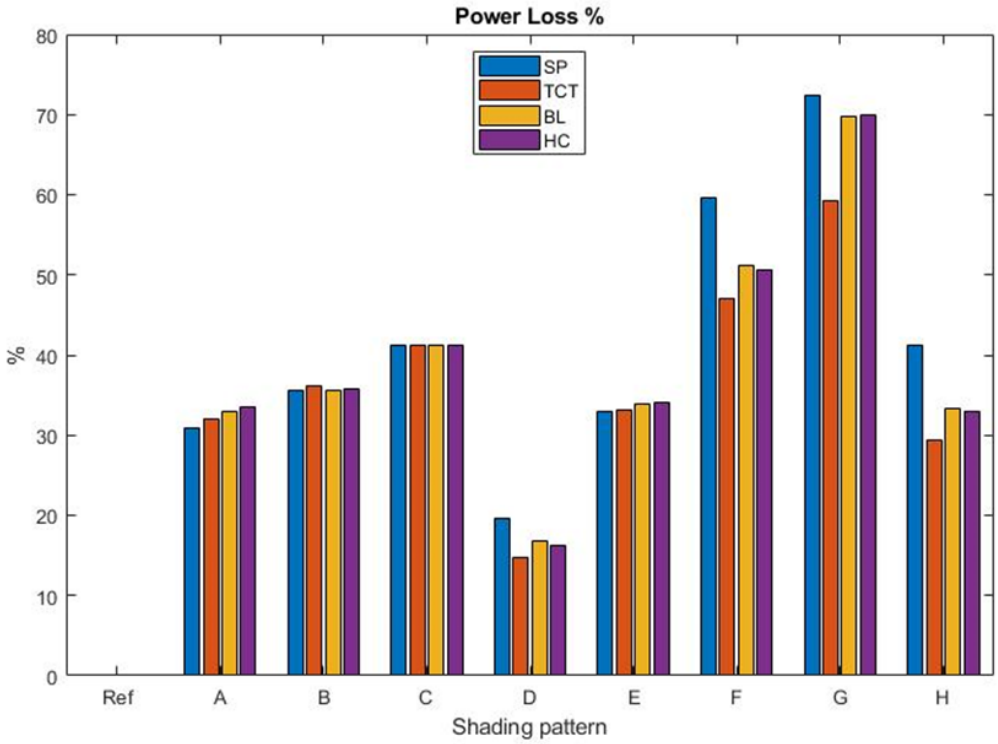

Figure 61 Power Loss Histogram (Lower is better)

III.4.2 Fill factor (FF)

FF is the ratio of generated MPP to the product of VOC and ISC. If FF is closer to unity then the PV system has better performance.

$$FF = \frac{MPP}{V_{OC} \times I_{SC}}$$

Where:

V_{OC} and I_{SC} are the open and short circuit voltage and currents of the PV array.

In figure 62, we notice that the Fill Factor FF is very irregular, this is due to the shading that covers parts of the GPV. Therefore, this factor is quite low for some scenarios, however the TCT configuration remains the best in these cases.

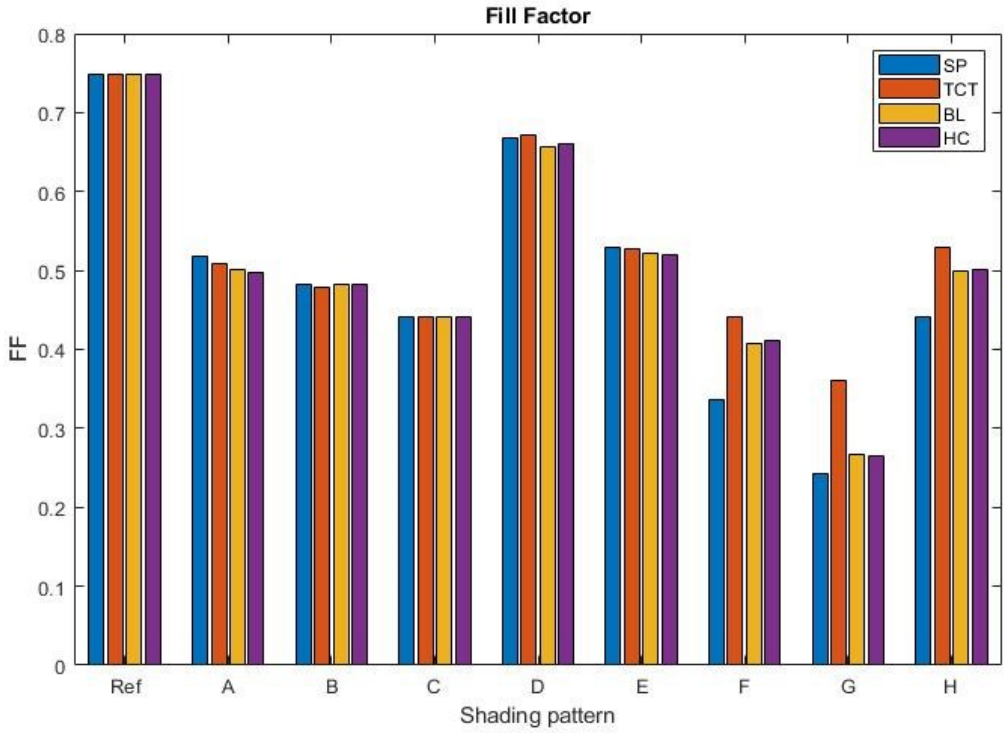

Figure 62 Fill Factor Histogram (Higher is better)

III.4.3 Synthesis

From all the simulation done before we can make a global analysis. Using FF and loss factor can give us a general view of the performance of each configuration regarding each scenario, but in real GPV operating, shading can be irregular and functioning point can be located every ware in the I-V curve.

This is why the results must be put into perspective, because certain situations are not visible in the histograms of figure 61 and figure 62. And it is clearly seen that all tested configurations can be efficient in certain regions of the I-V characteristics and less in others.

To solve this problem, we should analyze the functioning of these configurations over time, using dynamic simulations.

III.5 Dynamic algorithm design

For a dynamic photovoltaic generator, we need two basic algorithms, to observe the generator and when detecting a power loss only then the optimization algorithm is executed. the next flowcharts illustrated in figure 63 and figure 64 describe the observation and optimization algorithms

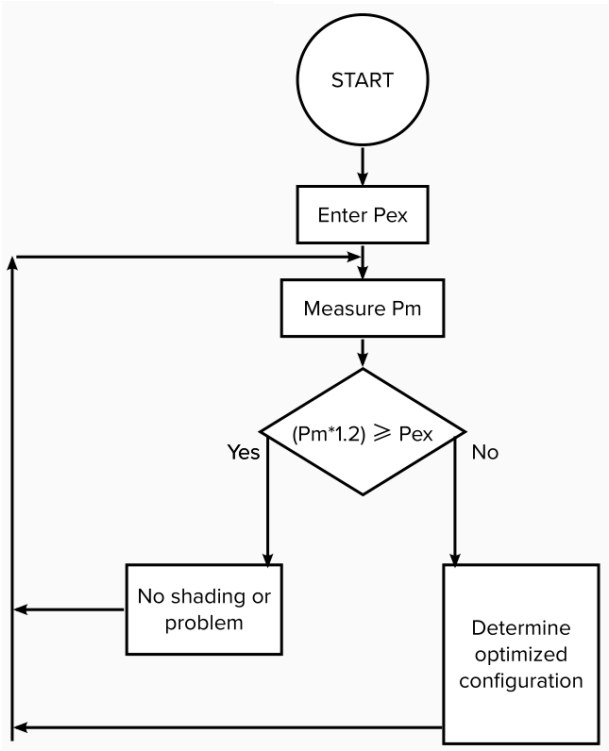

Figure 63 Observation algorithm flowchart

The objective of the observation algorithm is to determine whether yes or no the PV generator is providing the maximum power possible. This is done by measuring the actual power value and compare with the theoretical one.

This algorithm is only for demonstration, other wise we have to make a complex algorithm that determines the defect, give its category then to estimate its location.

The figure 64 illustrate the algorithm allow the GPV to change the configuration dynamically when the observation algorithm deliver a decision to optimize the layout of the PV array. The present algorithm changes the 4 available configuration and to chose the one that give the maximum power to the load.

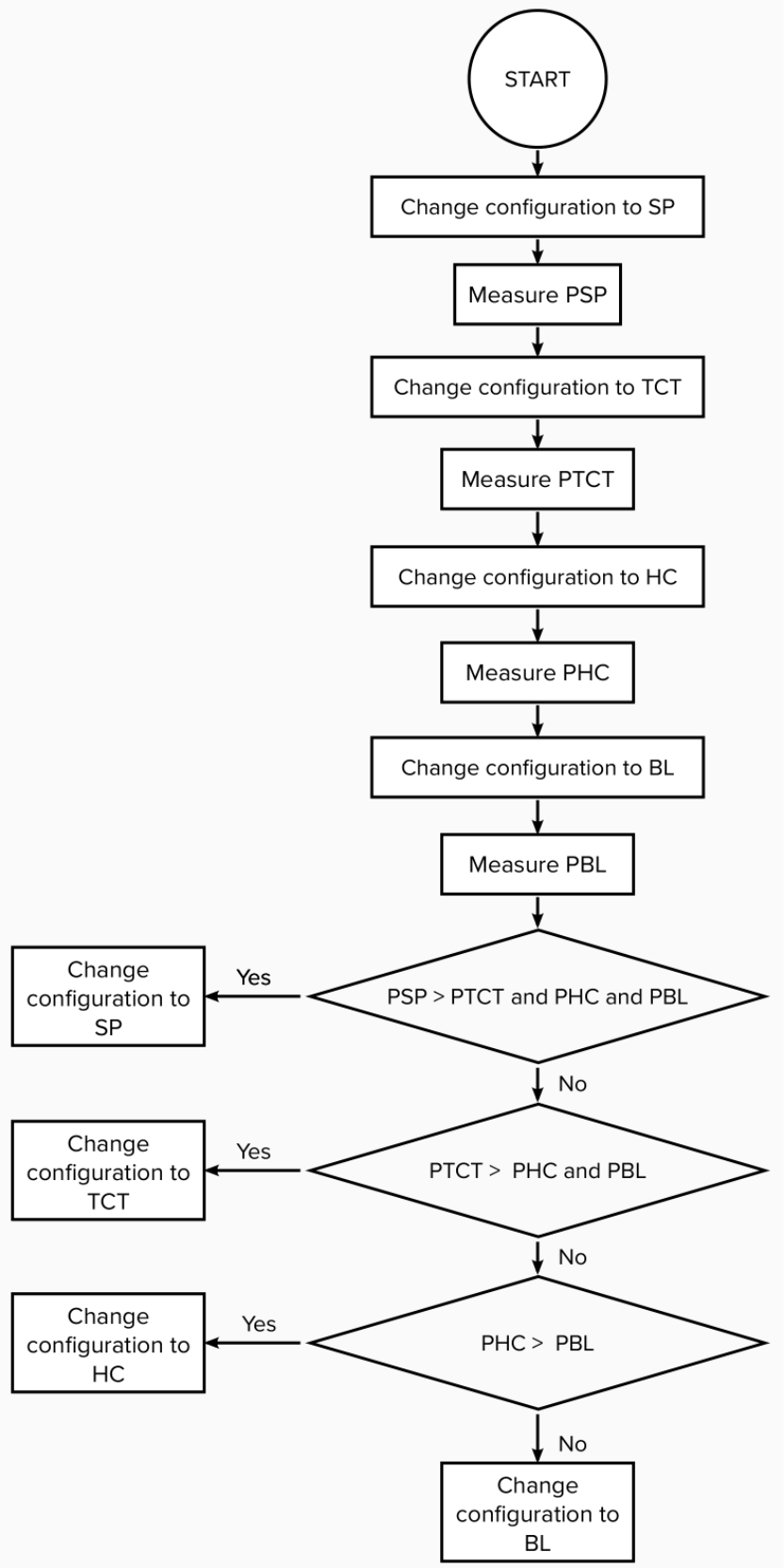

Figure 64 Optimization algorithm

III.6 Dynamic simulation

In dynamic simulation we choose a specific value for our load to demonstrate the effectiveness of reconfigurable generators during three different partial shading scenarios. While we set the scenario, we change the configuration successively and then the algorithm set the one with the maximum power.

Table 12 Dynamic model properties

Model properties	
Applied scenarios	E-L shape shading F- Frame shading H- Diagonal shading
Panels temperature	25 c
Load type	Resistor
Panels model	YL250P-29b 250W
Panels number	20 Panels
Bypass diodes	20 diodes, 1 diode each panel
Breakers number	12 breakers

Table 13 Dynamic simulation time settings

Time settings	
Simulation duration	3 s
Each topology duration	0.5 s
Best topology duration	1 s
The chosen topology time interval	[2 ; 3]

Table 14 Dynamic simulation time arrangement

Topologies arrangement		
Topology Order	Time Interval	Topology
1	[0 ; 0.5]	Serial Parallel (SP)
2	[0.5 ;1]	Totally Cross Tied (TCT)
3	[1 ; 1.5]	Bridge Linked (BL)
4	[1.5 ; 2]	Honey Comb (HC)

III.6.1 L-Shape shading R1

Table 15 Dynamic simulation results for R1 under L-shape scenario

Simulation results under L shape shading for R1		
R1 value	6.624 ohm	
Best topology	Bridge Linked (BL)	
Voltage [V]	SP	134.7
	TCT	134.3
	BL	**135.5**
	HC	134.7
Current [A]	SP	20.34
	TCT	20.28
	BL	**20.46**
	HC	20.34
Power [W]	SP	2741
	TCT	2724
	BL	**2773**
	HC	2740

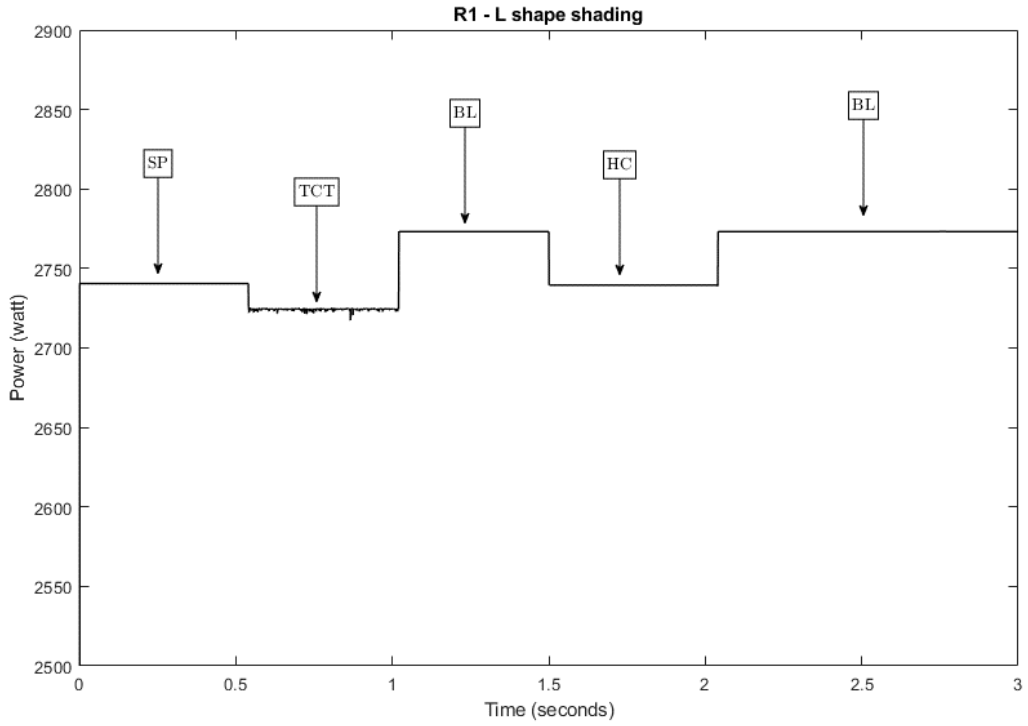

Figure 65 R1 Power curve under L-shape scenario

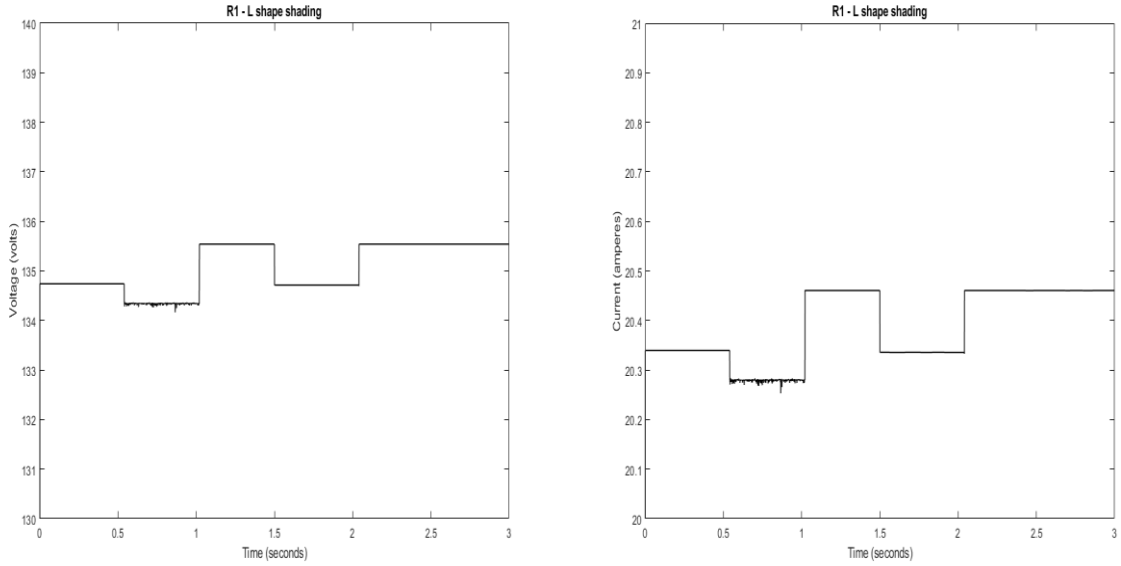

Figure 66 R1 Voltage and current curves under L-shape scenario

We imposed on the reconfigurable photovoltaic generator a shape shading and attached it to a charge (R = 6.624 ohm), we applied the four topologies to it, and through our observation of the power output, we found that BL is the best topology for this charge under this partial shading condition.

III.6.2 L-Shape shading R2

Table 16 Dynamic simulation results for R2 under L-shape scenario

Simulation results under L shape shading for R2		
R2 value	3.244 ohm	
Best topology	Series Parallel (SP)	
Voltage [V]	**SP**	**97.5**
	TCT	90.59
	BL	91.63
	HC	90.72
Current [A]	**SP**	**30.05**
	TCT	27.93
	BL	28.25
	HC	27.97
Power [W]	**SP**	**2930**
	TCT	2530
	BL	2588
	HC	2537

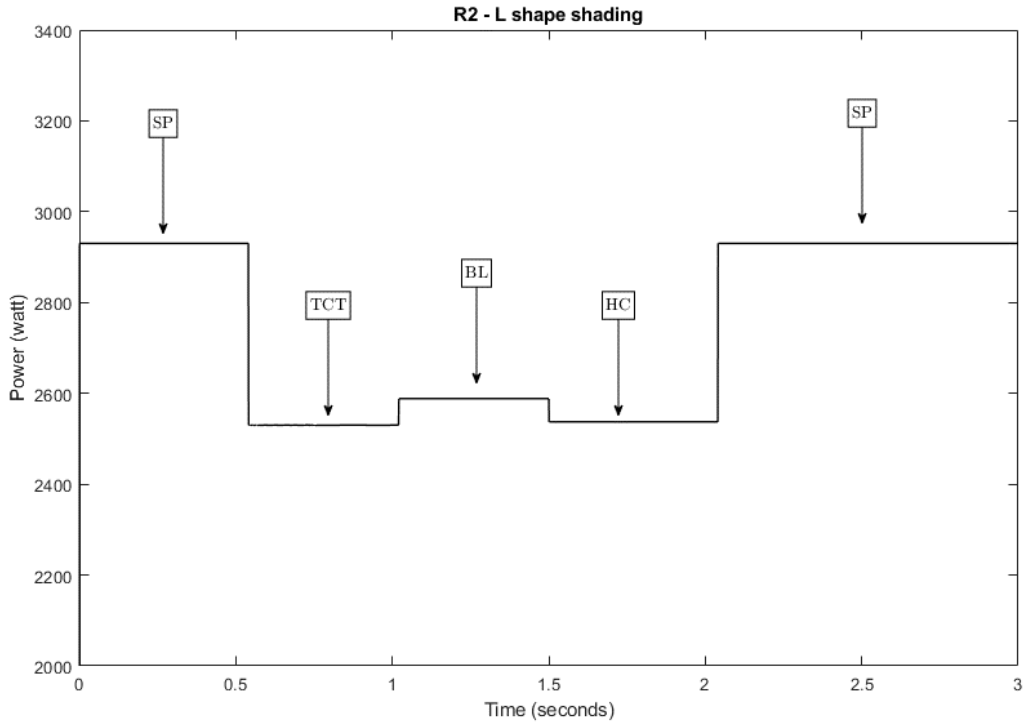

Figure 67 R2 Power curve under L-shape scenario

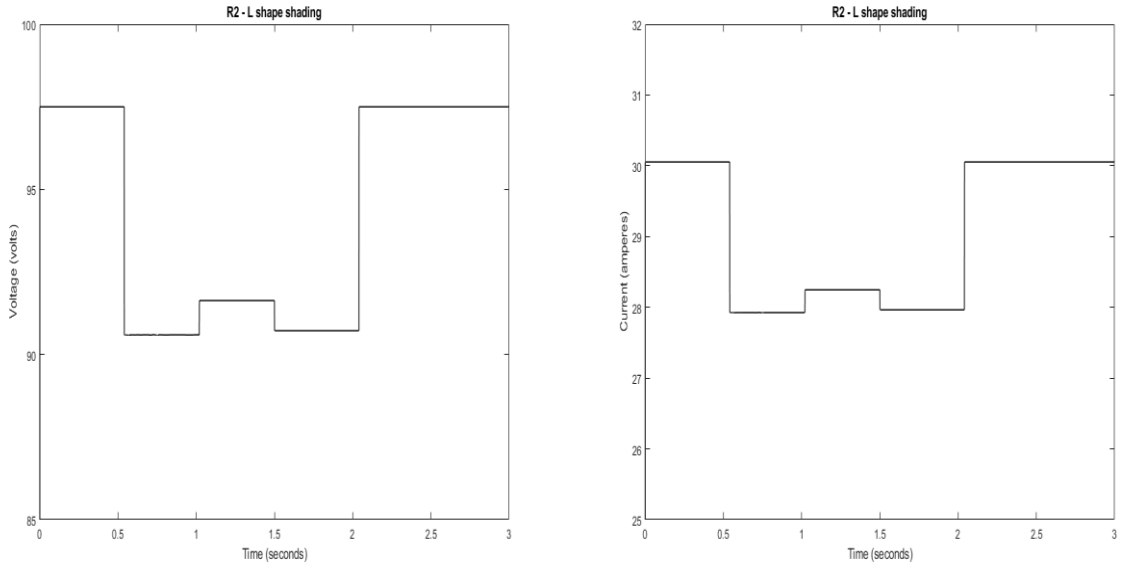

Figure 68 R2 Voltage and current curves under L-shape scenario

We changed the charge at this stage (R = 3 .244 ohm) and did the same previous steps, but this time we found that SP is the optimal topology (P=2930w).

III.6.3 Frame shading R1

Table 17 Dynamic simulation results for R1 under Frame shading scenario

Simulation results under Frame shading for R1		
R1 value	10.082 ohm	
Best topology	Totally Cross Tied (TCT)	
Voltage [V]	SP	134.8
	TCT	**160.7**
	BL	154.6
	HC	155.1
Current [A]	SP	13.37
	TCT	**15.94**
	BL	15.33
	HC	15.38
Power [W]	SP	1803
	TCT	**2563**
	BL	2370
	HC	2386

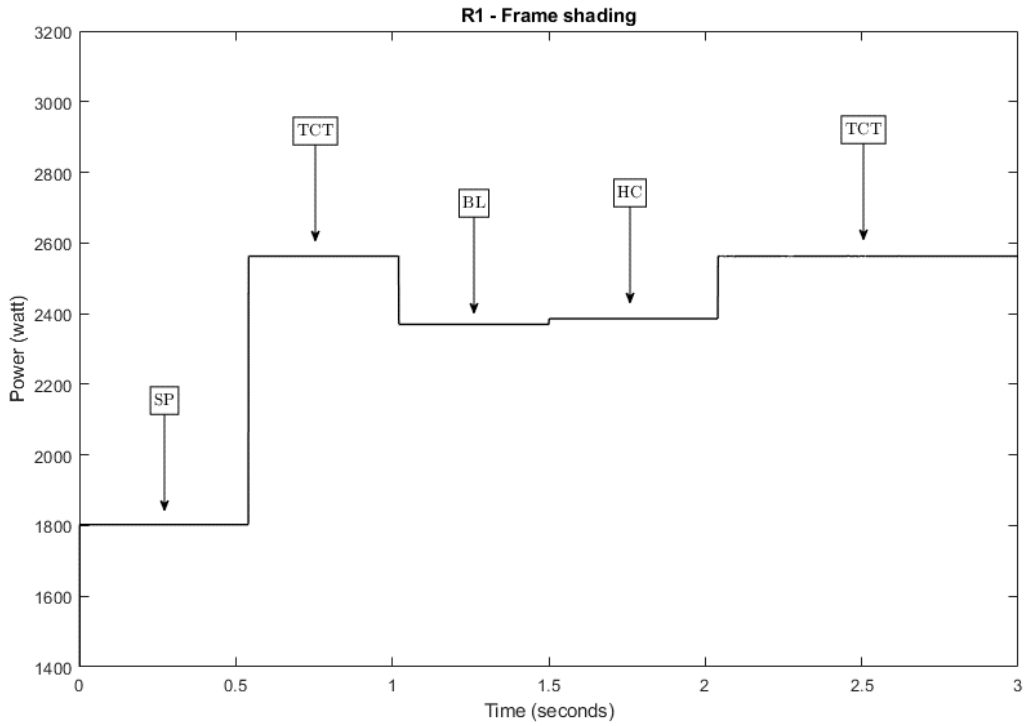

Figure 69 R1 Power curve under Frame shading scenario

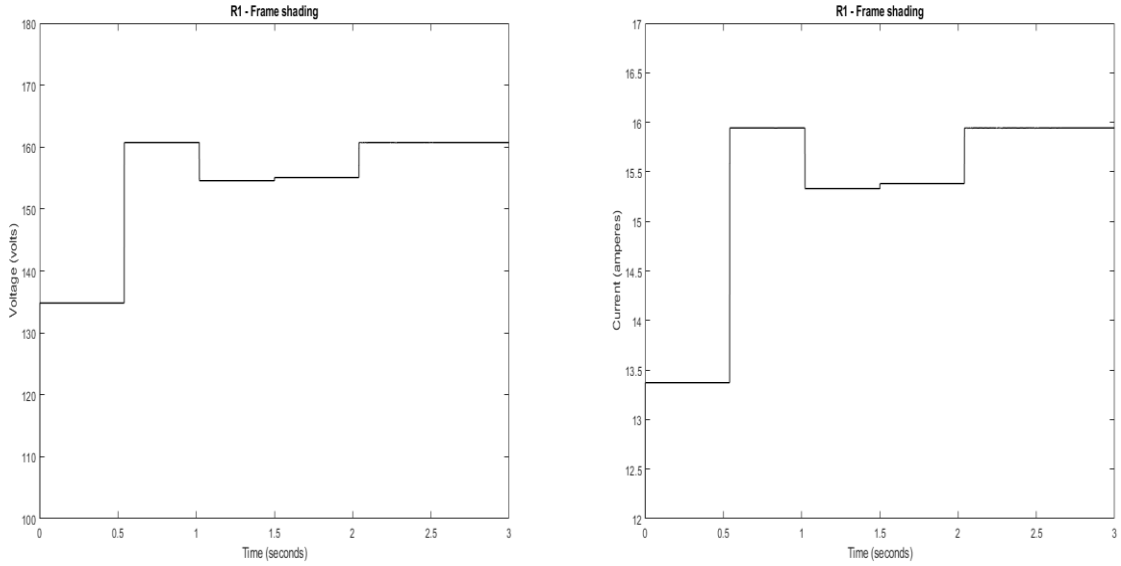

Figure 70 R1 Voltage and current curves under Frame shading scenario

We imposed on the reconfigurable photovoltaic generator a frame shading and attached a charge (R = 10.082 ohm), we applied the four topologies to it, and through our observation of the power output (P=2563w), we found that TCT is the best topology for this charge under these conditions.

III.6.4 Frame shading R2

Table 18 Dynamic simulation results for R2 under Frame shading scenario

Simulation results under Frame shading for R2		
R2 value	2.135 ohm	
Best topology	Series Parallel (SP)	
Voltage [V]	**SP**	**59.14**
	TCT	54.25
	BL	54.41
	HC	52.23
Current [A]	**SP**	**27.69**
	TCT	25.4
	BL	25.48
	HC	24.46
Power [W]	**SP**	**1638**
	TCT	1378
	BL	1386
	HC	1277

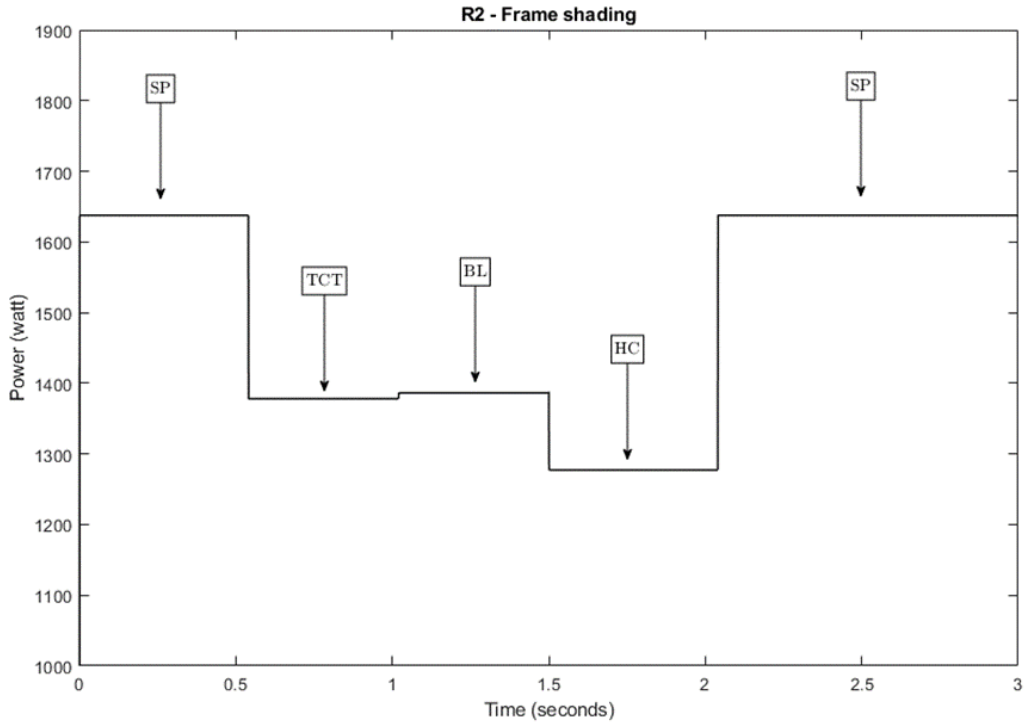

Figure 71 R2 Power curve under Frame shading scenario

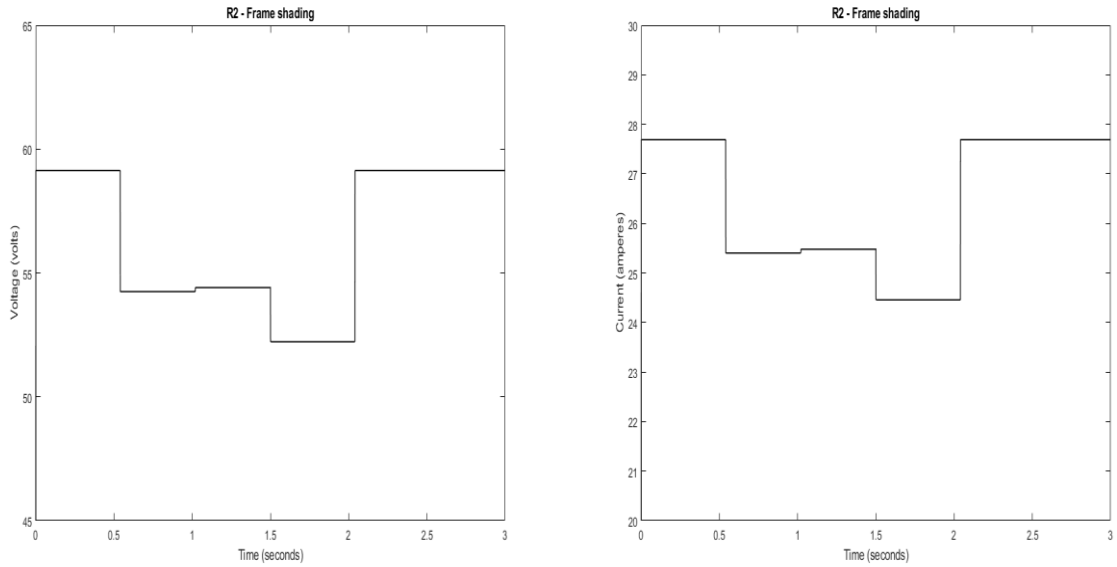

Figure 72 R2 Voltage and current curves under Frame shading scenario

At this stage, we changed the charge where we put (R=2.135 ohm) and applied the four topologies, and through our observations of the power (P=1638 w) , we concluded that SP is the best topology that achieves the maximum power.

III.6.5 Diagonal shading R1

Table 19 Dynamic simulation results for R1 under Diagonal shading scenario

Simulation results under Diagonal shading for R1		
R1 value	4.685 ohm	
Best topology	Honey Comb (HC)	
Voltage [V]	SP	102.8
	TCT	118.5
	BL	123.8
	HC	**124.1**
Current [A]	SP	21.94
	TCT	25.29
	BL	26.42
	HC	**26.48**
Power [W]	SP	2255
	TCT	2996
	BL	3271
	HC	**3284**

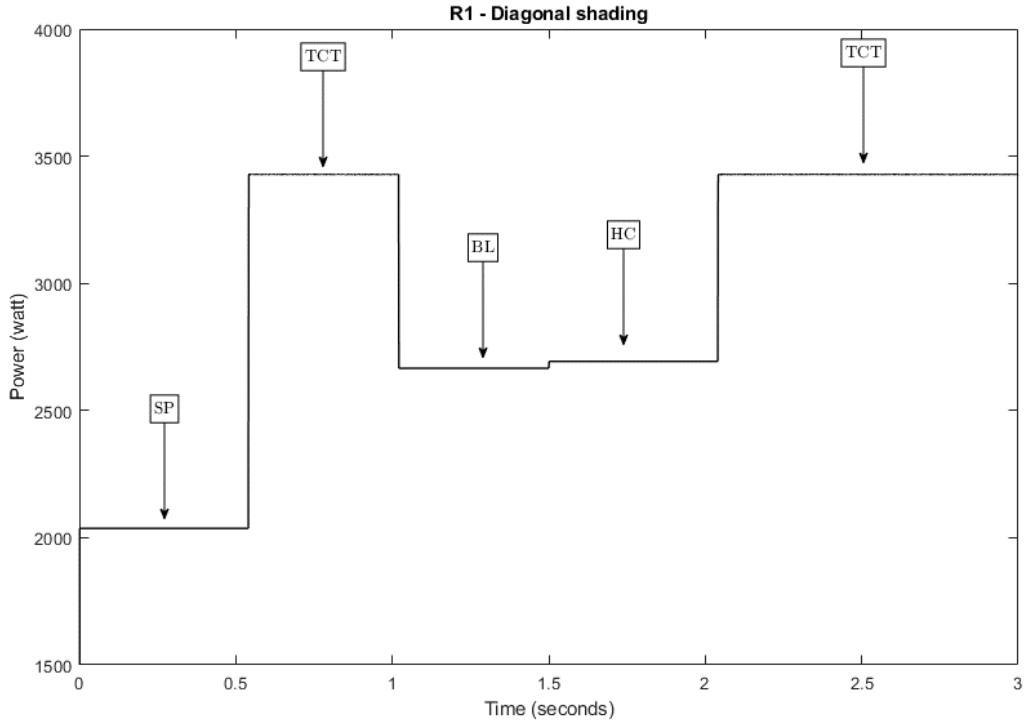

Figure 73 R1 Power curve under Diagonal shading scenario

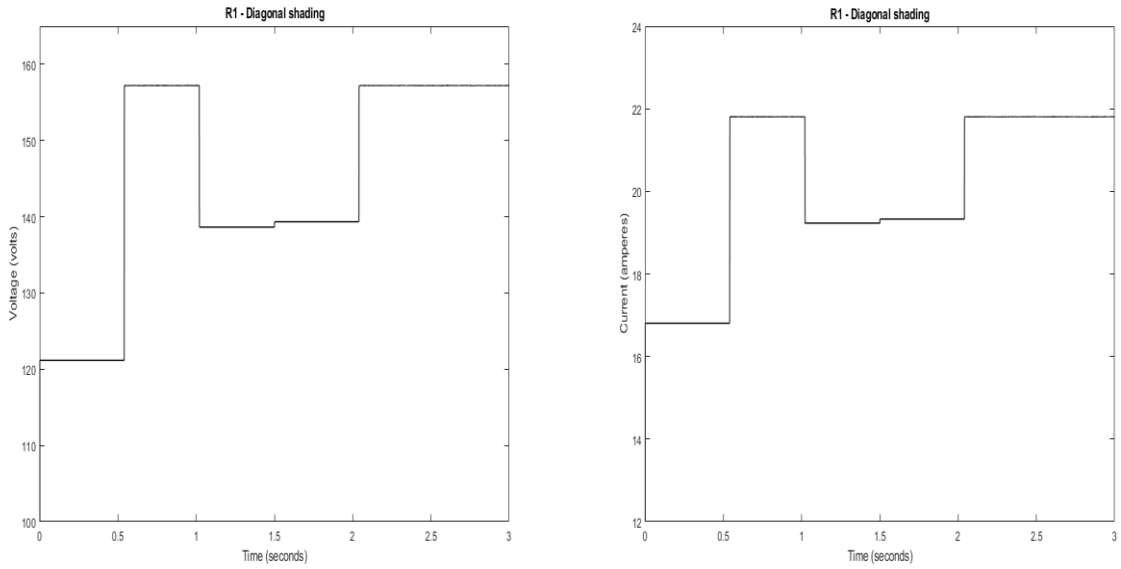

Figure 74 R1 Voltage and current curves under Diagonal shading scenario

We imposed on the reconfigurable photovoltaic generator a diagonal shading and attached it to a charge (R = 4.685ohm); we applied the four topologies to it, and through our observation of the maximum power (P=3283w), we observed that HC is the best topology for this charge.

III.6.6 Diagonal shading R2

Table 20 Dynamic simulation results for R2 under Diagonal shading scenario

Simulation results under Diagonal shading for R2		
R2 value	7.209 ohm	
Best topology	Totally Cross Tied (TCT)	
Voltage [V]	SP	121.2
	TCT	**157.2**
	BL	138.6
	HC	139.3
Current [A]	SP	16.81
	TCT	**21.81**
	BL	19.23
	HC	19.33
Power [W]	SP	2036
	TCT	**3428**
	BL	2666
	HC	2693

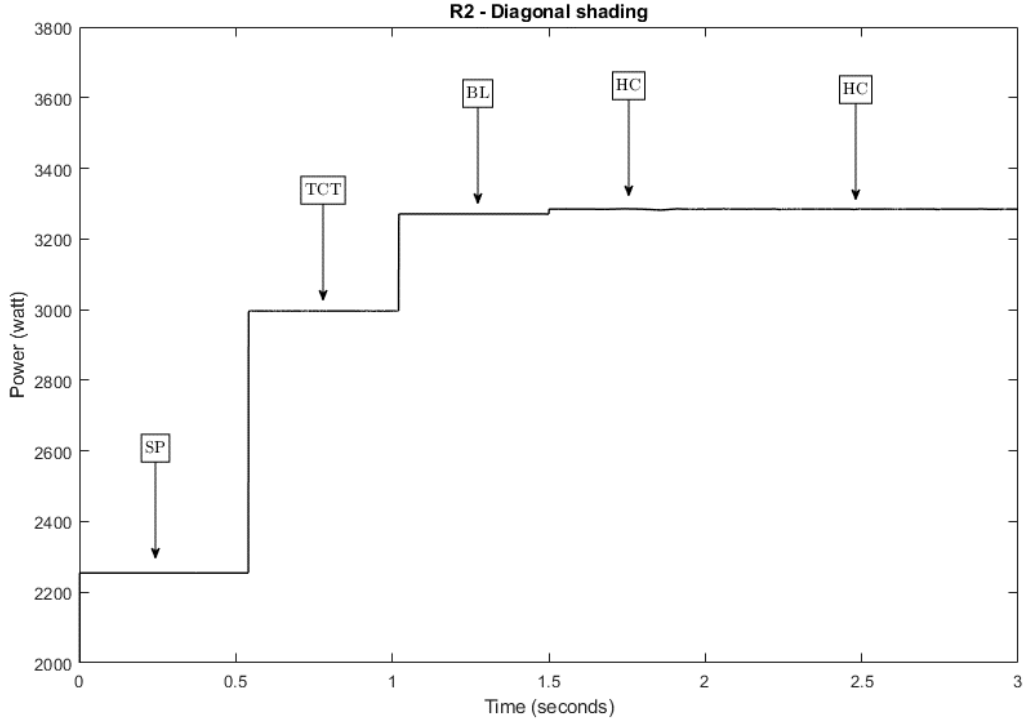

Figure 75 R2 Power curve under Diagonal shading scenario

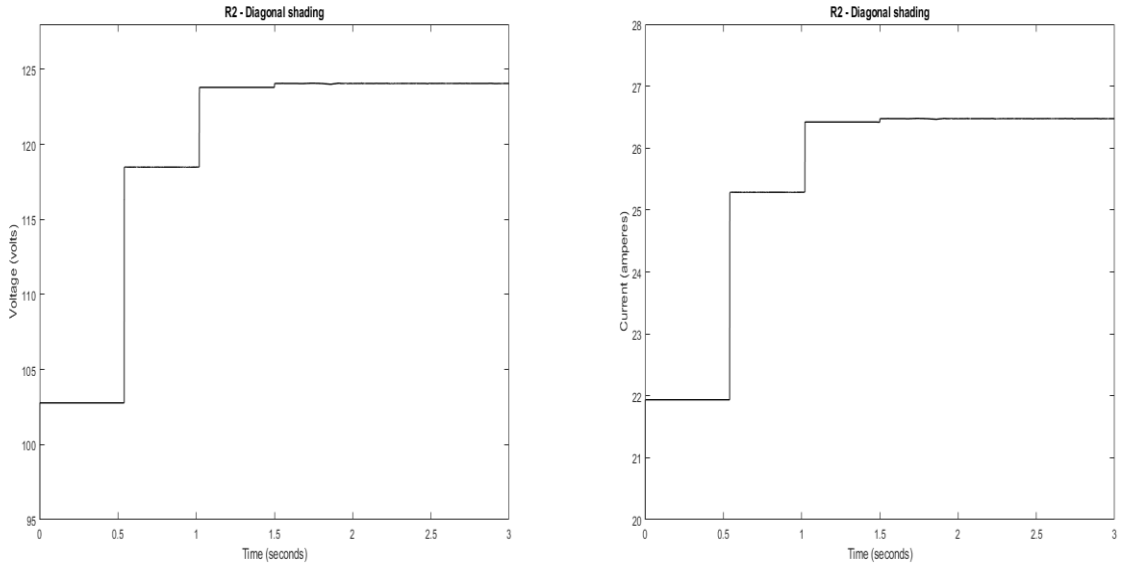

Figure 76 R2 Voltage and current curves under Diagonal shading scenario

In the second stage of this scenario, we changed the charge (R=7.209) and applied the same steps as the first stage. We noticed that the maximum power (P=3428 w) is due to the TCT topology.

III.7 Conclusion

In this chapter, we present a simulation model that has eight scenarios in the case of different partial shading experiences, to see the characteristics of each scenario and the effectiveness of the reconfigurable structures in optimally operating the photovoltaic system. We also put forward the various factors that affect the performance of PV array configurations.

A static simulation to see the characteristics of each scenario and the effectiveness of the reconfigurable structures in optimally operating the photovoltaic system. We also put forward the various factors that affect the performance of PV array configurations.

A dynamic simulation under different scenarios and different loads to achieve the best topology under a specific load and partial shading conditions.

Through these various experiments, we conclude that each for each case and for each condition we have a specific configuration that achieves maximum power extracting.

General conclusion

Solar power plants suffer from partial shading and mismatch problems, also the generation of hotspots and the resulting security problems. A reconfigurable photovoltaic generator was proposed to overcome these problems. Reconfigurable systems change the interconnection between solar modules to match the requirements of the system, this interconnection is composed of a matrix of switches that can evolve dynamically during system run.

In our work, we propose to use a PV generator with reconfigurable capability, the proposed system is composed of 20 PV modules drawing approximatively 5000Watts and the matrix switch accumulate 12 controllable switches. The reconfiguration scheme is used to find the optimal array topology under shading conditions. An ideal PV array connected in any topology performs identically. When faults occur in the array, the performance of each topology differs and the array does not produce the maximum yield. In this work, reconfiguration method is proposed to predict the optimal topology for a photovoltaic array consisting of shaded modules. To perform a dynamically reconfigurable ability we control the switch matrix using an adapted algorithm

This method of reconfiguration requires a specific algorithm to control the switch matrix. Therefore, we propose a simplified algorithm that estimate the current power then apply a new configuration that is adapted to the actual situation.

In this manuscript, we present the design and the simulation of the proposed system. To verify and validate the present method, we achieve tow kind of simulation.

The first is static: the system has been exposed to different scenario of shading for all possible topologies.

The second is dynamic: we have adopted a specific scenario and applied an algorithm to perform a simplified method of optimization. This method tests the different topology and choose the best one to reach the highest possible power.

The presented results show the effectiveness of the proposed work, but some limitations have to be exanimated and removed, this will improve the operational performance of the system through the robustness of the control method.

References:

[1] P. S. Vicente, E. M. Vicente, and E. R. Ribeiro, “A review of solar photovoltaic array reconfiguration methods,” *IEEE Int. Symp. Ind. Electron.*, vol. 2015-Septe, pp. 208–213, 2015, doi: 10.1109/ISIE.2015.7281470.

[2] H. K. V Lotsch *et al.*, *Optical Sciences*. 2007.

[3] P. J. Tulpule, V. Marano, S. Yurkovich, and G. Rizzoni, “Economic and environmental impacts of a PV powered workplace parking garage charging station,” *Appl. Energy*, vol. 108, pp. 323–332, 2013, doi: https://doi.org/10.1016/j.apenergy.2013.02.068.

[4] A. Luque and S. Hegedus, *Handbook of Photovoltaic Science and Engineering*. 2011.

[5] H. Wirth, *Harry Wirth Photovoltaic Module Technology*. .

[6] N. Enebish, D. Agchbayar, S. Dorjkhand, D. Baatar, and I. Ylemj, “Numerical analysis of solar cell current-voltage characteristics,” *Sol. Energy Mater. Sol. Cells*, vol. 29, no. 3, pp. 201–208, 1993, doi: https://doi.org/10.1016/0927-0248(93)90035-2.

[7] D. S. H. Chan and J. C. H. Phang, “Analytical methods for the extraction of solar-cell single- and double-diode model parameters from I-V characteristics,” *IEEE Trans. Electron Devices*, vol. 34, no. 2, pp. 286–293, 1987, doi: 10.1109/T-ED.1987.22920.

[8] R. Messenger and J. Ventre, *Photovoltaic Systems Engineering, Third Edition*. 2010.

[9] M. Z. Olindo Isabella, Klaus Jäger, Arno Smets, René van Swaaij, *Solar Energy - The Physics and Engineering of Photovoltaic Conversion, Technologies and Systems*. UIT Cambridge (Ltd), 2016.

[10] S. Silvestre, A. Boronat, and A. Chouder, “Study of bypass diodes configuration on PV modules,” *Appl. Energy*, vol. 86, no. 9, pp. 1632–1640, 2009, doi: https://doi.org/10.1016/j.apenergy.2009.01.020.

[11] W. Herrmann, W. Wiesner, and W. Vaassen, “Hot spot investigations on PV modules-new concepts for a test standard and consequences for module design with respect to bypass diodes,” in *Conference Record of the Twenty Sixth IEEE Photovoltaic Specialists Conference - 1997*, 1997, pp. 1129–1132, doi: 10.1109/PVSC.1997.654287.

[12] S. Rogotis, D. Ioannidis, A. Tsolakis, and D. Tzovaras, “Early defect diagnosis in installed PV modules exploiting spatio-temporal information from thermal images,” 2014, doi: 10.21611/qirt.2014.038.

[13] I. A. Karim, “Fault analysis and detection techniques of solar cells and PV modules,” in *2015 International Conference on Electrical Engineering and Information Communication Technology (ICEEICT)*, 2015, pp. 1–4, doi: 10.1109/ICEEICT.2015.7307349.

[14] Y. El Basri and Y. El Basri, “Architecture de puissance distribuée reconfigurable dédiée à l’optimisation de l’énergie photovoltaïque.”

[15] D. La Manna, V. L. Vigni, E. Riva, V. Di Dio, and P. Romano, “Recon fi gurable electrical interconnection strategies for photovoltaic arrays : A review,” vol. 33, pp. 412–426, 2014.

[16] R. Ramaprabha and B. L. Mathur, “A comprehensive review and analysis of solar

photovoltaic array configurations under partial shaded conditions," *Int. J. Photoenergy*, vol. 2012, 2012, doi: 10.1155/2012/120214.

[17] S. Ferguson, A. Siddiqi, K. Lewis, and O. L. de Weck, "Flexible and Reconfigurable Systems: Nomenclature and Review," *33rd Des. Autom. Conf.*, vol. 6, pp. 249–263, 2007.

[18] K. A. H. Lakshika, M. A. K. S. Boralessa, M. K. Perera, D. P. Wadduwage, V. Saravanan, and K. T. M. U. Hemapala, "Reconfigurable solar photovoltaic systems: A review," *Heliyon*, vol. 6, no. 11, 2020, doi: 10.1016/j.heliyon.2020.e05530.

[19] H. Ertl, J. W. Kolar, and F. C. Zach, "A novel multicell DC-AC converter for applications in renewable energy systems," *IEEE Trans. Ind. Electron.*, vol. 49, no. 5, pp. 1048–1057, 2002, doi: 10.1109/TIE.2002.803212.

[20] D. D. Nguyen, "Modeling and reconfiguration of solar photovoltaic arrays under non-uniform shadow conditions Modeling and Reconfiguration of Solar Photovoltaic Arrays under Non-Uniform Shadow," *Electr. Eng.*, 2008.

[21] N. Chang, M. Pedram, H. G. Lee, Y. Wang, and Y. Kim, "Reconfigurable Photovoltaic Array Systems for Adaptive and Fault-Tolerant Energy Harvesting," doi: 10.1007/978-94-017-9990-4.

[22] X. Lin, Y. Wang, and M. Pedram, "Designing Fault-Tolerant Photovoltaic Systems," pp. 1–7.

[23] L. Ortiz, J. W. González, L. B. Gutierrez, and O. Llanes-Santiago, "A review on control and fault-tolerant control systems of AC/DC microgrids," *Heliyon*, vol. 6, no. 8, 2020, doi: 10.1016/j.heliyon.2020.e04799.

[24] H. Braun *et al.*, "Topology reconfiguration for optimization of photovoltaic array output," *Sustain. Energy, Grids Networks*, vol. 6, no. February, pp. 58–69, 2016, doi: 10.1016/j.segan.2016.01.003.

[25] P. K. Bonthagorla and S. Mikkili, " Performance analysis of PV array configurations (SP , BL , HC and TT) to enhance maximum power under non-uniform shading conditions ," *Eng. Reports*, vol. 2, no. 8, 2020, doi: 10.1002/eng2.12214.

[26] A. A. Desai and S. Mikkili, "Modelling and analysis of PV configurations (alternate TCT-BL, total cross tied, series, series parallel, bridge linked and honey comb) to extract maximum power under partial shading conditions," *CSEE J. Power Energy Syst.*, vol. PP, no. 99, 2019, doi: 10.17775/CSEEJPES.2020.00900.

[27] P. O. Singh, "Modeling of Photovoltaic Arrays under Shading Patterns with Reconfigurable Switching and Bypass Diodes," The University of Toledo, 2011.